Real-time Monitoring and Prediction of Tropical Cyclone AMPHAN: Satellite Perspective

SAC/EPSA/AOSG/ASD/SR-38/2020

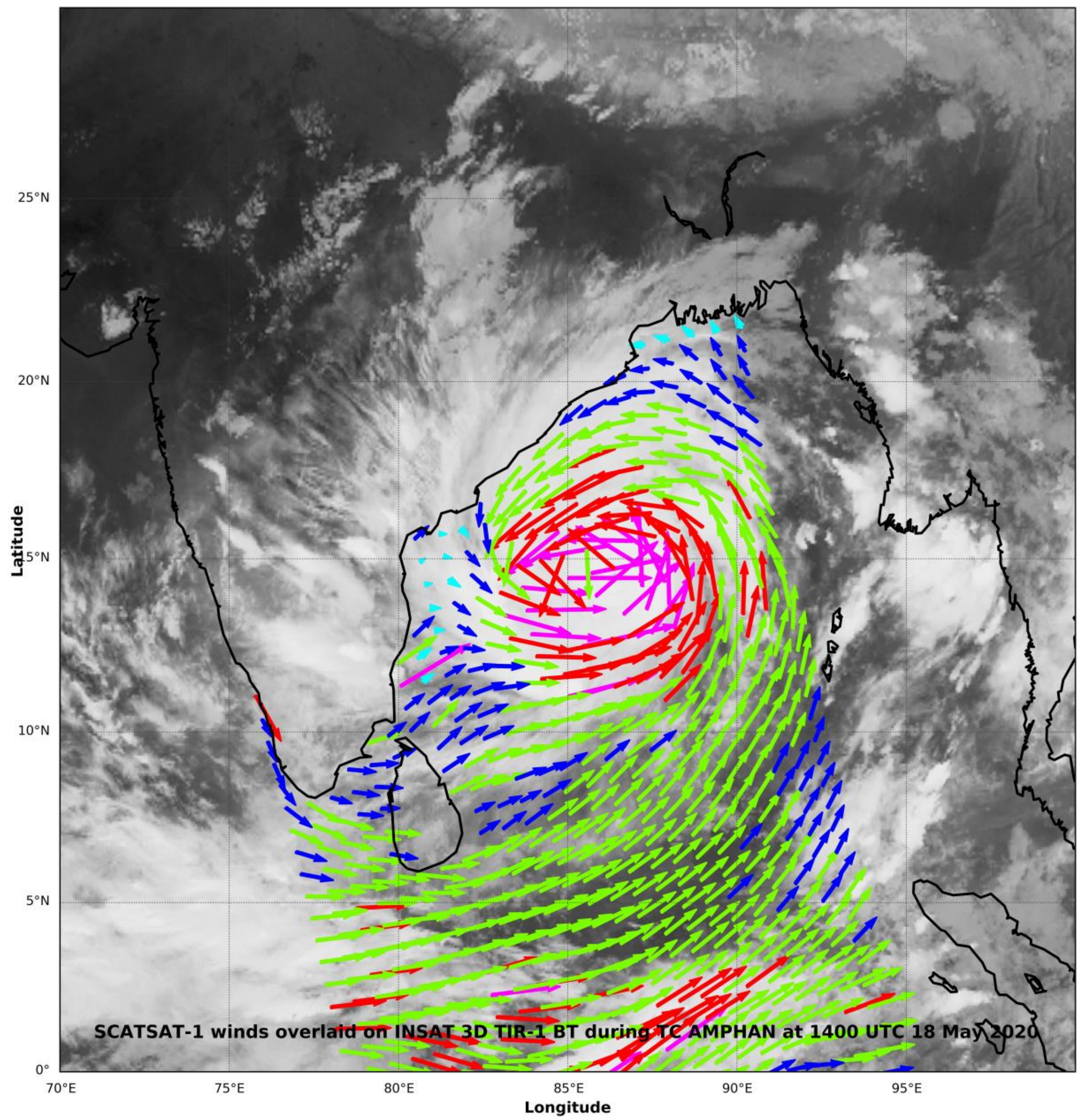

JUNE 2020

Atmospheric and Oceanic Sciences Group
Space Applications Centre (ISRO)
Ahmedabad-380015

Document Control and DATA Sheet

Report No.	SAC/EPSA/AOSG/ASD/SR/38/2020
Date	June, 2020
Title	Real-time monitoring and prediction of tropical cyclone AMPHAN: A satellite Perspective
Type of Report	Scientific Report
No. of Pages	45
Authors	Neeru Jaiswal, Shivani Shah, C. M. Kishtawal, R. M. Gairola
Number of Figures	19
Number of Tables	7
Number of References	20
Originating Unit	AOSG/EPSA/SAC
Abstract	The accurate and timely advance prediction of tropical cyclones is very important to disseminate the warnings and preparedness. Prediction of development of any cyclone system in the North Indian Ocean is being done at Space Applications Centre (ISRO) Ahmedabad, using the in-house developed algorithms. Once the low pressure system is formed, it is continuously monitored by satellite observations. The tropical cyclone track is predicted and updated. These forecasts and satellite based cyclone inputs are disseminated through web-portal SCORPIO linked to MOSDAC. The real-time prediction of cyclone AMPHAN and its structural analysis using satellite observations are presented in this report. The surface wind observations over TC AMPHAN by different satellites e.g. SCATSAT-1, CYGNSS, WINDSAT and SMAP are also presented in this report.
Key words	Tropical cyclone, track prediction, cyclogenesis, center determination, satellite observations
Security classification	Unrestricted

Acknowledgements

The authors are thankful to the Director, Space Applications Centre (ISRO), Ahmedabad and the Deputy Director of EPSA, SAC-ISRO. The authors acknowledge the Joint Typhoon Warning Centre (JTWC) and Regional Specialized Meteorological Centre (RSMC) for tropical cyclones over North Indian Ocean, India Meteorological Department (IMD), Delhi for providing real time cyclone track through their websites. IMD is also acknowledged for providing the best track estimates for TC AMPHAN. The satellite observations of SCATSAT, INSAT-3D and INASAT-3DR were obtained from MOSDAC (www.mosdac.gov.in). The satellite observations of WINDSAT and CYGNSS were obtained from PO-DAAC NASA website (https://podaac.jpl.nasa.gov/). SMAP products have been obtained from REMSS website (ftp://ftp.remss.com/smap/wind/).

Table of Contents

1. INTRODUCTION 5

1.1. OVERVIEW OF TROPICAL CYCLONE AMPHAN (16 - 20 MAY 2020) 5

2. DATA AND METHODOLOGY 8

2.1 TROPICAL CYCLOGENESIS PREDICTION 8
2.2 CYCLONE TRACK PREDICTION 9
2.2.1 SAC-Lagrangian Advection Model 9

3. RESULTS: PREDICTION OF TC AMPHAN 11

3.1 CYCLOGENESIS PREDICTION OF TC AMPHAN 11
3.2 REAL-TIME TRACK PREDICTION OF TC AMPHAN 13
3.3 INTENSITY PREDICTION OF TC AMPHAN 22
3.4 SHIP AVOIDANCE REGION PREDICTION FOR TC AMPHAN 23

4. SATELLITE OBSERVATIONS OVER TC AMPHAN 24

4.1 INSAT 3D PRODUCTS 24
4.2 INSAT-3DR RAPID SCAN OBSERVATIONS OVER TC AMPHAN 26
4.3 SATELLITE BASED SURFACE WIND OBSERVATIONS OVER TC AMPHAN 29
4.3.1 SCATSAT-1 29
4.3.2 CYGNSS 31
4.3.3 SMAP 33
4.3.4 WINDSAT 36
4.3.5 Comparison of Satellite Wind Speed Products 38

5. DISSEMINATION OF FORECASTS THROUGH WEB 39

6. CONCLUSIONS 42

REFERENCES 44

1. Introduction

Indian sub-continent is one of the most adversely affected cyclone active basins that experience on an average 4-5 cyclones every year. In comparison to other cyclone basins this region is the most vulnerable due to relatively dense coastal population, shallow bottom topography and coastal configuration. Though the cyclones formed in this region are considered to be weaker in intensity and smaller in size as compared to other regions, yet the number of deaths in the region is highest in the globe. To overcome such loss, advance prediction of cyclones in terms of their genesis, track and intensity is highly important. The timely prediction of impending cyclonic activity can save life of people and help in decision making for taking preventive measures like evacuation during the cyclone landfall. The predictions of TC are generated based on the models using satellite observations and ground based radar networks when cyclone reaches close to the land. Due to the advancements in numerical prediction models, computational resources and satellite observations with high temporal and spatial resolutions, during the last decades, the track prediction accuracy has improved drastically. However, the prediction of cyclogenesis and cyclone intensity is still challenging.

Prediction of development of any cyclone system in the North Indian Ocean (NIO) including the Bay of Bengal (BoB) and Arabian Sea is being done as a regular exercise at Space Applications Centre (ISRO) Ahmedabad, using the in-house developed algorithms. Once the system is developed in the NIO basin its track and intensity are predicted in real-time and disseminated through web-portal Satellite based cyclone real-time prediction in Indian Ocean (SCORPIO) linked to MOSDAC (www.mosdac.gov.in). The similar exercise was performed during the formation of cyclone "AMPHAN" in NIO during 13-20 May 2020, which has been discussed in the present report.

1.1. Overview of Tropical cyclone AMPHAN (16 - 20 May 2020)

The tropical cyclone "AMPHAN", was classified by IMD as Super cyclonic storm (SuCS). It was originated from a low pressure system formed in southeast area of Bay of Bengal on 14 May 2020. This well marked low pressure area concentrated into a depression over southeast Bay of Bengal on 16th May 2020. The depression intensified into a Deep Depression and lay centered over the same region at 09 UTC 16th May, 2020 near latitude 10.9°N and longitude 86.3°E. The deep depression remained practically stationary and rapidly intensified into a Cyclonic Storm 'AMPHAN' (pronounced as UM-PUN). It lay centered over the same region at 12 UTC 16th May, 2020 near latitude 10.9°N and longitude 86.3°E (Source: IMD Bulletins).

The Observed track of TC AMPHAN with its intensity categories provided by IMD has been shown in the Figure 1. The IMD classification of cyclone categories is given in Table 1.

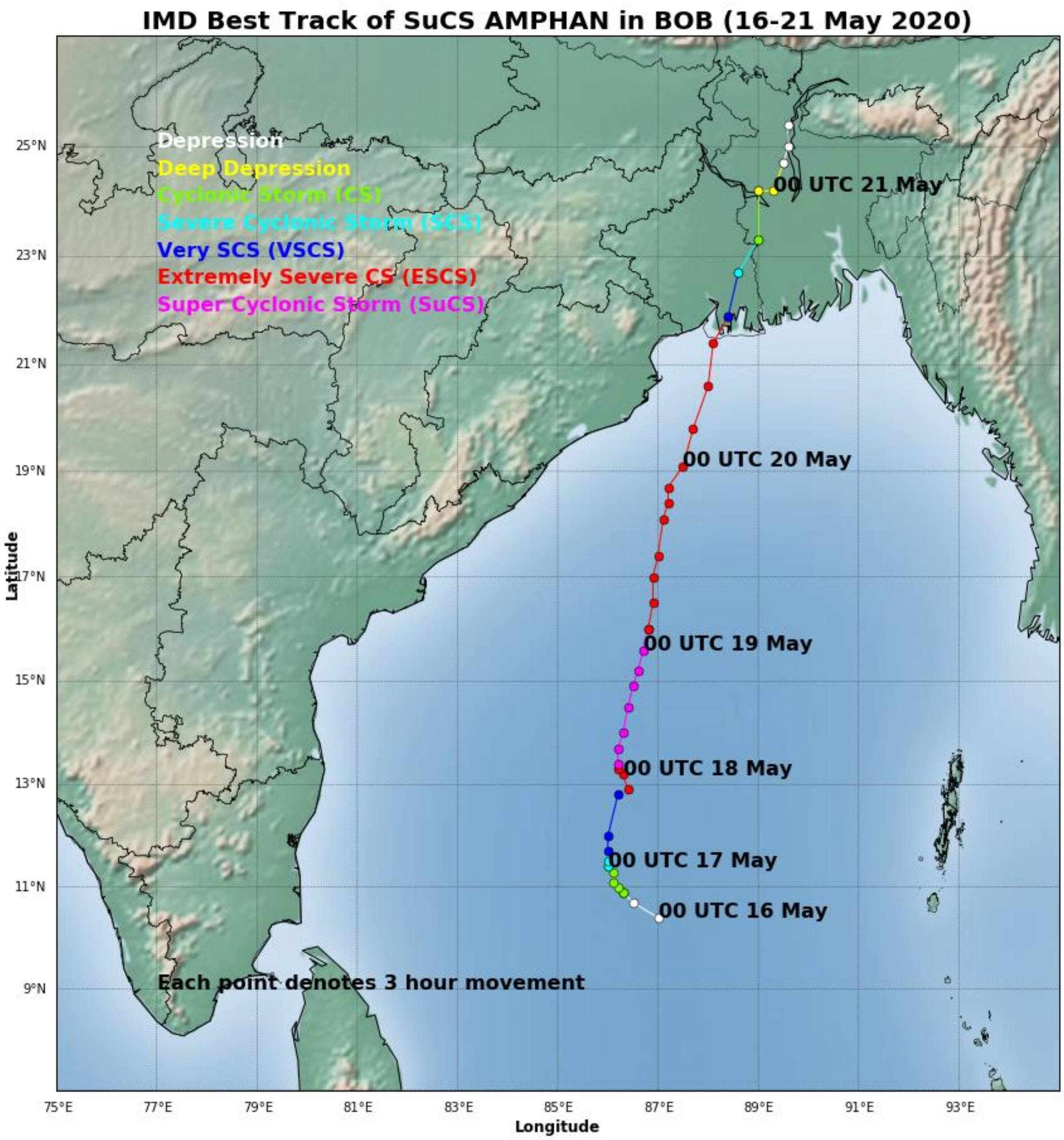

Figure 1: IMD best track of super cyclonic storm AMPHAN with its intensity categories.

Table 1: IMD classification tropical cyclone intensity categories

System	Associated wind speed (knots)
Low pressure area	<17
Depression	17-27
Deep Depression	28-33
Cyclonic Storm	34-47
Severe Cyclonic Storm (SCS)	48-63
Very SCS (VSCS)	64-85
Extremely SCS (ESCS)	86-119
Super Cyclonic Storm(SuCS)	>119

The cyclone name “AMPHAN”, was given by Thailand and means "sky". As per global convention, the eight countries that make up the Indian Ocean Region—India, Bangladesh, Sri Lanka, Thailand Pakistan, Maldives, Myanmar, Oman—have drawn up a list of names (in the year 2004) for tropical cyclones, which are assigned serially with the alphabetic order of the nation’s name.

Development stages of the cyclone AMPHAN were continuously monitored by the visible and infrared observations from Indian geo-stationary satellites viz., INSAT-3D, INSAT-3DR and high resolution microwave satellite SCATSAT-1. SCATSAT provided very good observations over these cyclonic systems, which were found to be very helpful for its prediction and structural analysis. The surface wind observations provided by advanced foreign satellites like CYGNSS, SMAP and WINDSAT have also been discussed in this report. Using the observations and models, the real-time predictions of cyclone track, intensity, rainfall and wind structure were performed at SAC-ISRO. The real-time prediction of the cyclone using in-house developed algorithms and the satellite observations over the system that helped in monitoring and prediction has been discussed in this report. The in-house developed techniques used for the cyclone prediction are briefly discussed in the section 2. The separate sections are made for the detail discussion of satellite estimated surface wind analysis and its comparison w.r.t IMD and JTWC estimates.

2. Data and Methodology

A system has been formed in the SAC to predict the cyclones from its birth till death. This starts with predicting the earliest signatures of development of a low pressure system i.e. tropical cyclogenesis. After the declaration of system as tropical cyclone or cyclonic storm by JTWC or IMD, its track is predicted and updated during the life period of the cyclone till its landfall occurs. The track prediction also includes its landfall time and position prediction. Predictions of cyclone intensity is also generated using NWP models. All these predictions are disseminated in the real-time through a web server "Satellite based cyclone observations and real-time prediction in Indian Ocean" i.e. SCORPIO linked with MOSDAC (www.mosdac.gov.in).

2.1 Tropical Cyclogenesis Prediction

A technique developed at Space Applications Centre based on the patterns of low level circulation using observations from scatterometer to determine the possibility of cyclogenesis over the Indian Ocean as well as other global basins has been used in this work (Jaiswal and Kishtawal, 2011). It is based on the assumption that there is some degree of similarity in low level wind circulation among the low pressure systems that could turn in tropical storm at later stages, which can be utilized to distinguish them from non-developing systems. First, a database was prepared containing such wind patterns of low level circulations that turn into TCs at later stage using the QuikSACT observations during the period 2000-09. The similarity of wind patterns in the database and real-time derived OSCAT winds were measured quantitatively using a Block Matching Algorithm (BMA). The matching between the vector fields was determined by considering them as complex variables, [*for example A = (u+iv)*]. The matching index (*c*) between the two sets of such complex numbers was computed as follows:

$$c = 1 - \frac{\frac{1}{N}\sum_{i=1}^{N}\left(\left|A_i - B_i\right|\right)^2}{\sqrt{\frac{1}{N}\sum_{i=1}^{N}\left(\left|A_i - \overline{A}\right|\right)^2} \times \sqrt{\frac{1}{N}\sum_{i=1}^{N}\left(\left|B_i - \overline{B}\right|\right)^2}} \tag{1}$$

where $\overline{A}$ and $\overline{B}$ represents the mean value of the complex vectors *A* and *B* respectively. *N* is the dimension of vector *A* (or *B*) which is the number of valid pairs between two scenes to be matched. The threshold of matching index was estimated as 0.6. The winds derived by SCATSAT-1 in each pass were matched with the scenes archived in the database and the value of the matching index is computed. If the matching index exceeds the threshold value the system is declared as the developing system and cyclogenesis is predicted.

2.2 Cyclone Track Prediction

After the formation of tropical cyclone in the North Indian Ocean, track predictions are carried out using in-house developed Lagrangian advection cyclone track prediction model (SAC-LAGAM). A brief summary of the model has been given in the following subsections.

2.2.1 SAC-Lagrangian Advection Model

SAC-Lagrangian Advection model is dynamical framework based computationally efficient model (Singh et al, 2011; 2012). It requires the high resolution 0.5^0 x 0.5^0 atmospheric winds and temperature forecasts from Global forecast System (GFS), which is global numerical weather prediction model run by NOAA, and the initial position of cyclone which is obtained from JTWC. The cyclone track prediction is provided using SAC- Lagrangian Advection model up to 96 hour with 6 hour interval. As a first step, the steering flow has been computed for every 6-hour forecast interval up to 96 hours, using the analysis as well as forecast wind fields data at 21 pressure levels (100-1000 mb) by the weighted average scheme. The weight for each level was assigned by estimating the potential vorticity (PV) which is adapted from the study by Hoover et al., 2006. Then a cyclonic vortex is removed using a synthetic cyclone which is constructed by using the vorticity equation (Chan and Williams, 1987):

$$\frac{\partial \zeta}{\partial t} + V.\nabla(\zeta + f) = 0$$

Where ζ is the vorticity and $f = \beta y + f_0$. Here y denotes latitudinal displacement, f_0 is the value of coriolis parameter at y = 0 and β is the rate of change of coriolis parameter with latitude. In case of axisymmetric vortex, the velocity is calculated using the equation (Chan and Williams, 1987):

$$V(r) = V_m\left(\frac{r}{r_m}\right)\exp\left[\frac{1}{b}\left(1-\left(\frac{r}{r_m}\right)^b\right)\right]$$

Where V_m and r_m denote the maximum value of tangential velocity and the radius at which V_m occurs, respectively. This synthetic cyclone was used to remove the existing cyclonic wind fields present in the steering flow to achieve the residual steering current. To avoid the discontinuity of wind fields due to removal of cyclonic circulation, tapered weights *W (k)* are used for generation of residual flow fields. Now, resulting steering flow that is obtained after removing the cyclonic vortex from steering flow is used in model to forecast the cyclone track. The computation for the trajectory of the cyclone (or the cyclone track) is initiated by interpolating the steering wind from model grid points to the initial location of the cyclone (Brand, 1981).

The above discussed techniques and models, which are used in the real-time for the prediction of cyclone AMPHAN.

3. Results: Prediction of TC AMPHAN

Real-time cyclogenesis and track prediction of TC AMPHAN was carried out at SAC using the above discussed algorithms. The results of real-time prediction and the validation of the forecasts have been discussed in this section.

3.1 Cyclogenesis prediction of TC AMPHAN

The real-time generated SCATSAT-1 ocean surface winds during the cyclogenesis stage of TC AMPHAN have been shown in the Figure 2. The presence of low pressure system at south east BoB was captured by SCATSAT-1 on 12th May morning pass (01:42 UTC). This system was continuously watched and the indication of its development into cyclone was earliest detected on 14 May morning pass (01:42 UTC) as the cyclogenesis algorithm showed the wind pattern matching index 0.65 which was higher than predetermined threshold for cyclogenesis i.e.0.6. Thus, the earliest cyclogenesis of TC AMPHAN was determined on 14 May 2020. The cyclone was declared as cyclonic storm on 12 UTC 16 May by IMD as it achieved intensity of 35 knots. The lead prediction time of tropical cyclogenesis prediction of TC AMPHAN was 58 hours.

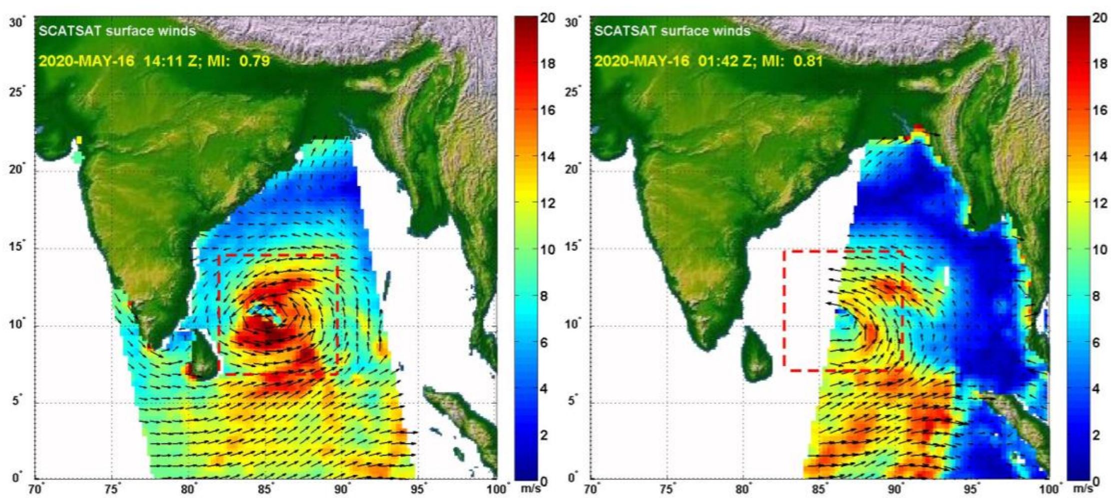

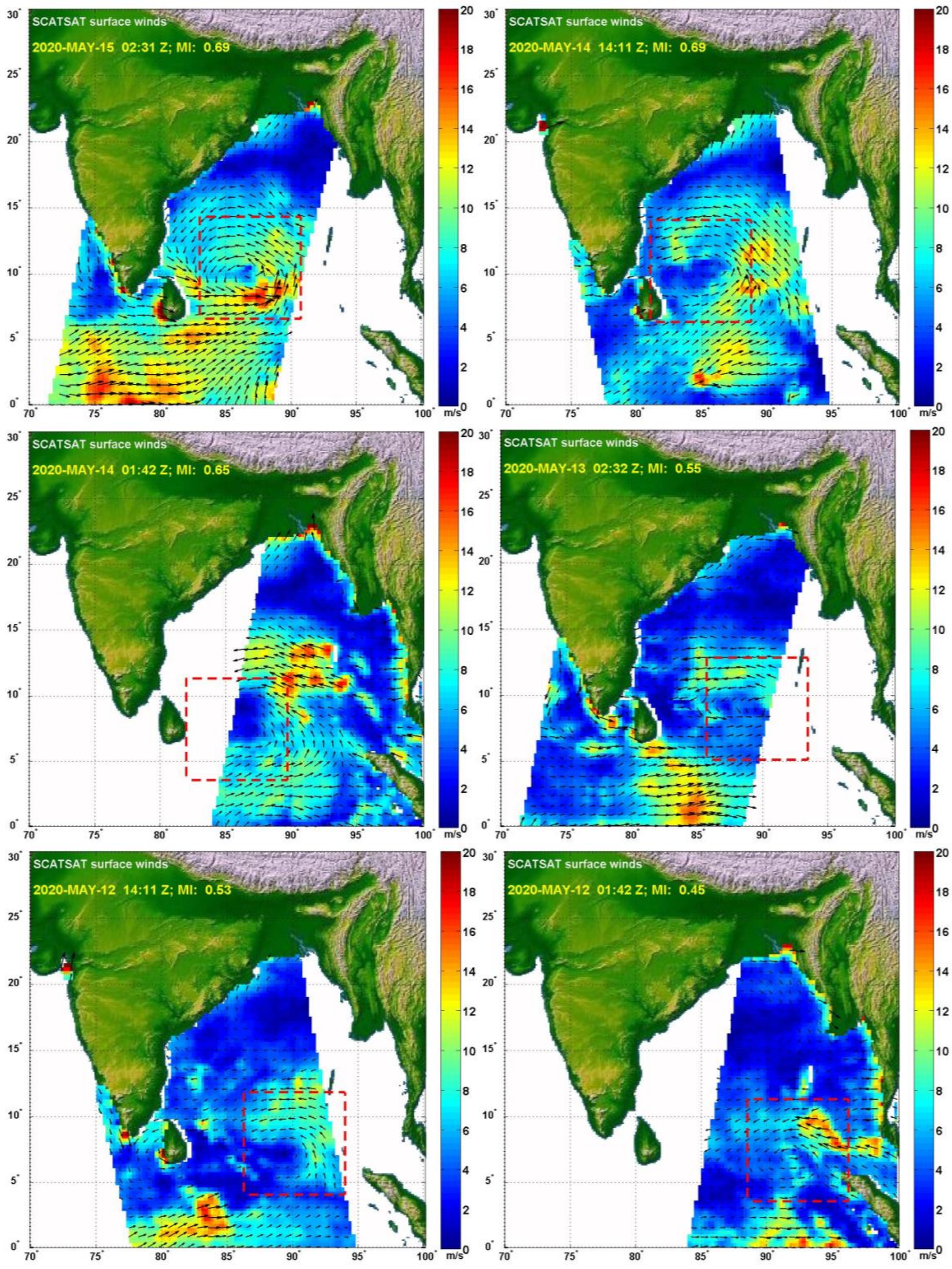

Figure 2: SCATSAT-1 winds over the bay of Bengal during genesis of TC AMPHAN

3.2 Real-time track prediction of TC AMPHAN

After formation of TC AMPHAN its track was predicted using the SAC-Lagrangian Advection model. The cyclone track forecast using SAC-Lagrangian model was generated on 00, 06, 12 and 18 UTC of 16th -20th May 2020 and have been shown in the Fig. 3. The initial position of cyclone in the forecasts was taken from the real-time provided cyclone bulletins of JTWC. Each point in the figure is representing the six hours' movement of the cyclone. Each day forecasts have been presented in different colors with four different marker styles for four initial forecasts hours in a day. IMD best track and JTWC real-time observed track has also been presented in the figure.

In the real-time these tracks were disseminated over the website which have been provided in Fig. 4. Based on the past track error statistics of the model, the cone of uncertainty has been computed and shown as a shaded region along the predicted track.

The forecasted track were compared with JTWC observed track and the error of track forecast has been estimated. The direct position error (DPE), cross track (CT) and along track (AT) component of track forecast error were calculated with respect to JTWC observed track position values for all the forecasts generated on different initial conditions and have been given in the Table 2, 3, and 4, respectively. The schematic showing the computation of the track errors is shown in the Fig. 5.

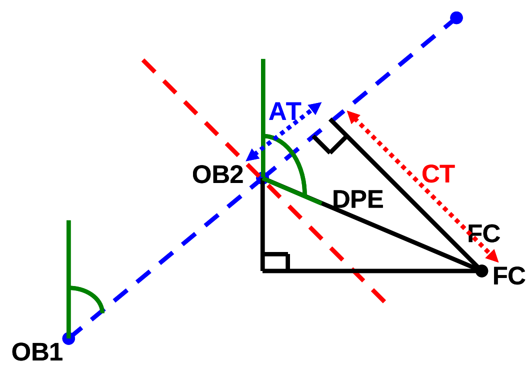

Figure 3: Schematic showing the positional forecast errors (Heming, 1994).

The position error of track forecast by SAC-model is also estimated w.r.t. IMD best track positions. The values have been summarized in the Table 5.

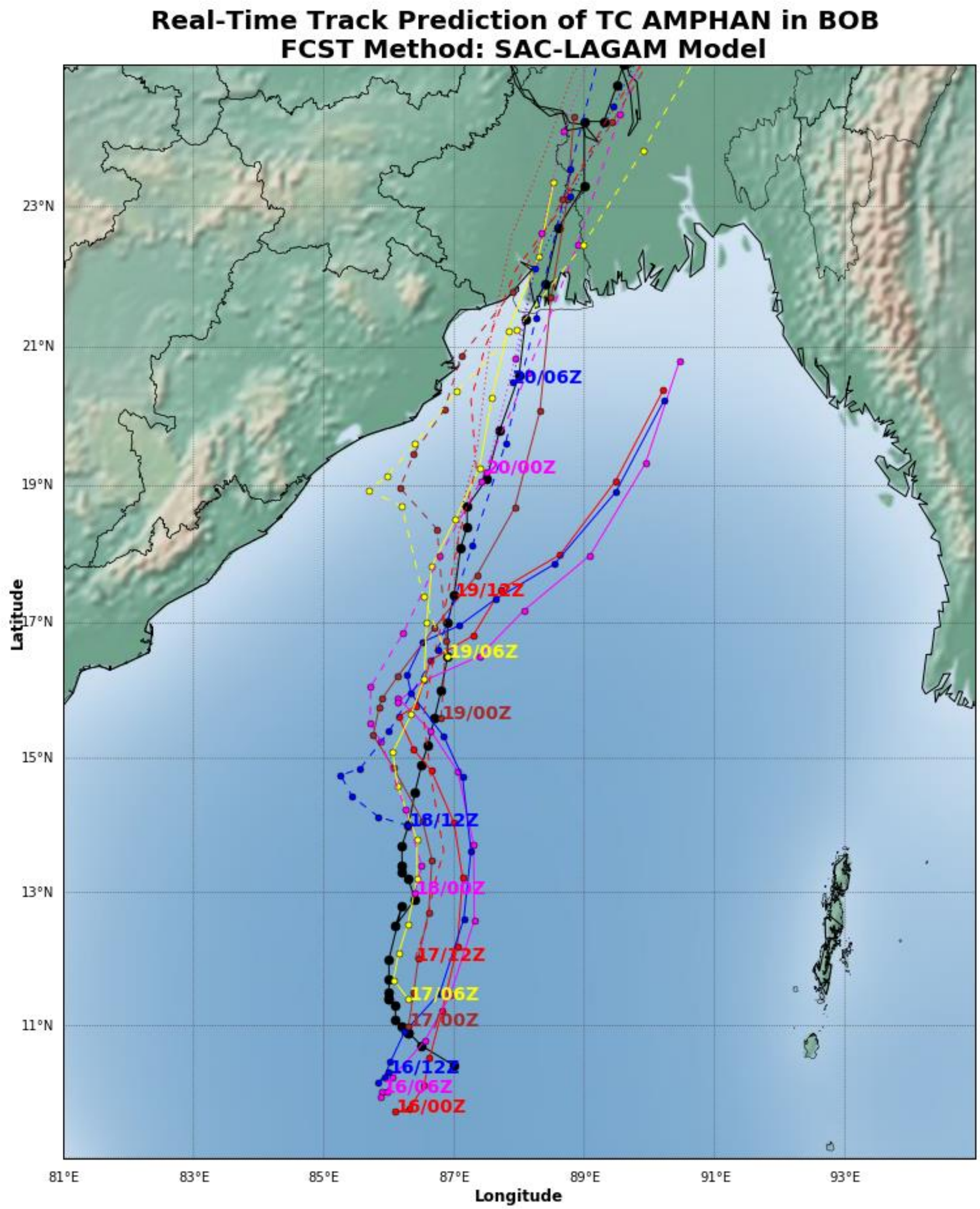

Figure 4a: Real-time predicted track of TC AMPHAN at 00, 06 and 12 UTC 16-20 May 2020 with the IMD best track.

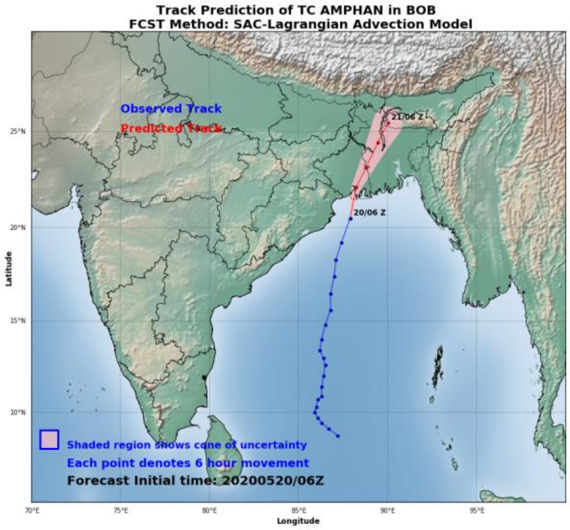
Track Prediction of TC AMPHAN in BOB
FCST Method: SAC-Lagrangian Advection Model
Observed Track
Predicted Track
21/06 Z
20/06 Z
Shaded region shows cone of uncertainty
Each point denotes 6 hour movement
Forecast Initial time: 20200520/06Z
Latitude
Longitude

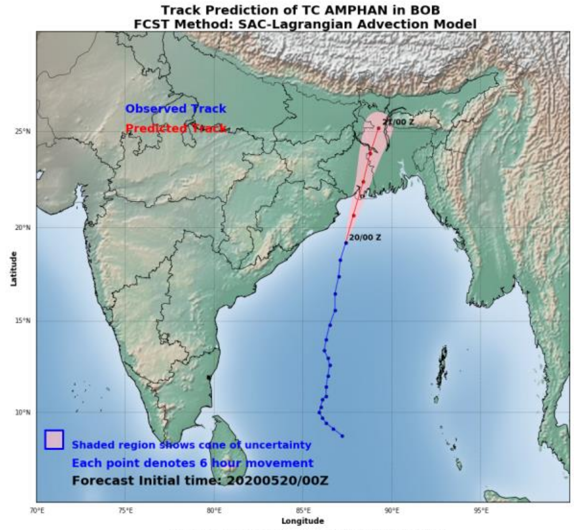
Track Prediction of TC AMPHAN in BOB
FCST Method: SAC-Lagrangian Advection Model
Observed Track
Predicted Track
21/00 Z
20/00 Z
Shaded region shows cone of uncertainty
Each point denotes 6 hour movement
Forecast Initial time: 20200520/00Z
Latitude
Longitude

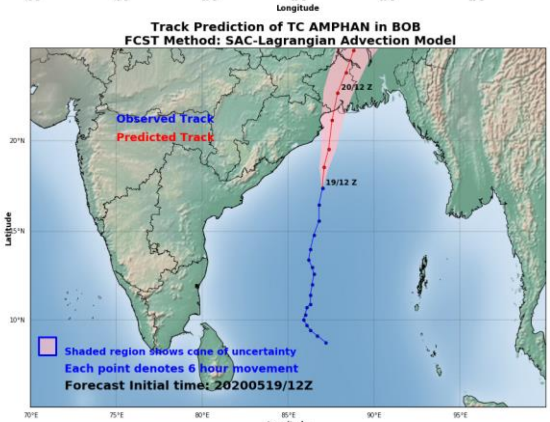
Track Prediction of TC AMPHAN in BOB
FCST Method: SAC-Lagrangian Advection Model
Observed Track
Predicted Track
20/12 Z
19/12 Z
Shaded region shows cone of uncertainty
Each point denotes 6 hour movement
Forecast Initial time: 20200519/12Z
Latitude
Longitude

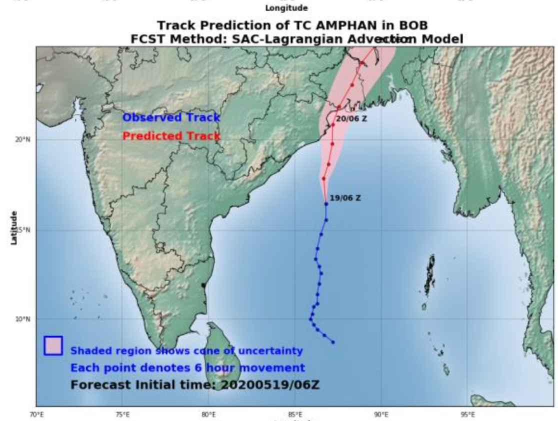
Track Prediction of TC AMPHAN in BOB
FCST Method: SAC-Lagrangian Advection Model
Observed Track
Predicted Track
20/06 Z
19/06 Z
Shaded region shows cone of uncertainty
Each point denotes 6 hour movement
Forecast Initial time: 20200519/06Z
Latitude
Longitude

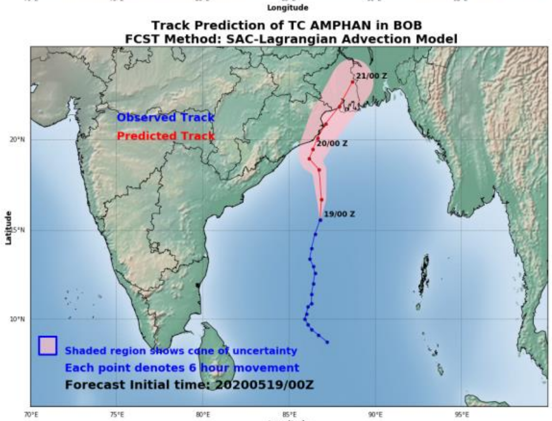
Track Prediction of TC AMPHAN in BOB
FCST Method: SAC-Lagrangian Advection Model
Observed Track
Predicted Track
21/00 Z
20/00 Z
19/00 Z
Shaded region shows cone of uncertainty
Each point denotes 6 hour movement
Forecast Initial time: 20200519/00Z
Latitude
Longitude

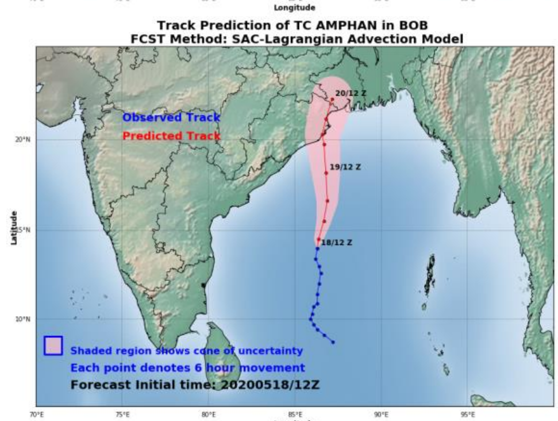
Track Prediction of TC AMPHAN in BOB
FCST Method: SAC-Lagrangian Advection Model
Observed Track
Predicted Track
20/12 Z
19/12 Z
18/12 Z
Shaded region shows cone of uncertainty
Each point denotes 6 hour movement
Forecast Initial time: 20200518/12Z
Latitude
Longitude

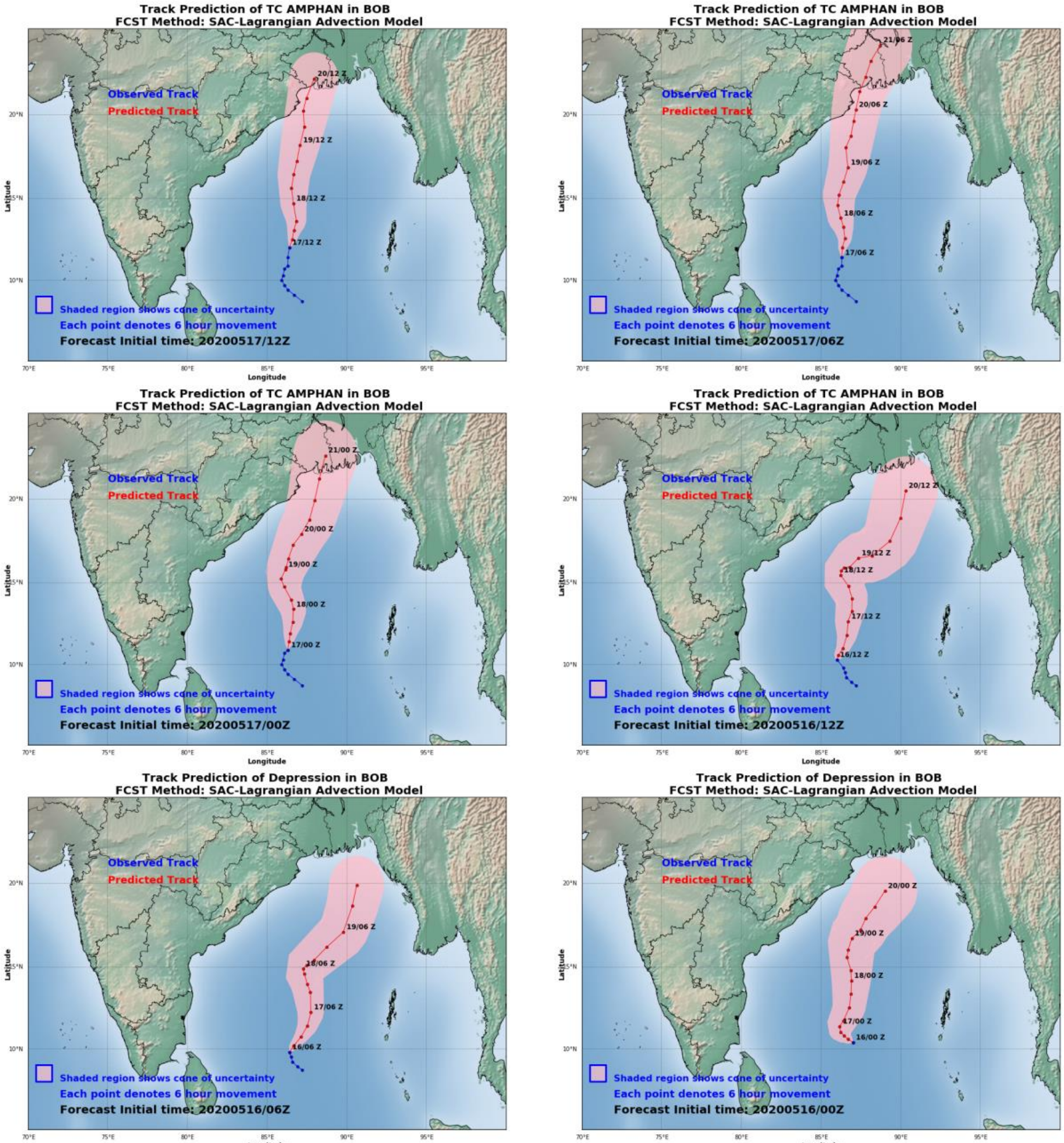

Figure 4b: Real-time predicted track of TC AMPHAN during 16-20 May, 2020.

Table 2: Direct position error of SAC-Lagrangian advection track prediction model for TC AMPHAN w.r.t JTWC real-time observed track

FCST Initial time	**Track Error (km) in different Forecast Lead time**															
	6	**12**	**18**	**24**	**30**	**36**	**42**	**48**	**54**	**60**	**66**	**72**	**78**	**84**	**90**	**96**
1600	53.76	63.14	60.63	62.23	119.92	158.05	169.01	204.17	193.34	180.86	108.29	96.05	53.98	77.03	165.07	208.5
1606	44.59	78.03	89.55	75.18	84.03	87.93	126.06	181.21	160.99	127.2	76.14	54.68	107.31	161.44	214.9	249.82
1612	68.92	94.69	109.97	122.45	127.13	92.16	117.19	120.01	69.32	63.45	72.64	91.22	149.02	206.24	301.15	385.18
1700	14.13	5.55	17.09	61.32	81.12	98.78	99.59	103.25	126.5	159.99	159.48	167.54	202.4	234.63		
1706	49.78	67.35	53.61	32.65	27.24	45.59	97.53	111.86	145.27	153.66	176.21	238.7	340.33			
1712	14.4	31.06	73.39	85.49	92.35	95.38	84.57	90.29	110.78	118.34	69.63	37.41				
1800	32.47	28.32	83.29	117.02	135.12	103.01	49.09	17.27	28.56	68.63						
1806	67.69	110.28	144.36	156.96	163.07	123.05	105.87	125.18	160.62							
1812	102.96	195.66	262.12	322.58	343.05	299.8	271.44	292.83								
1900	25.66	111.31	123.09	121.29	118.19	192.41										
1906	49.92	104.81	192.4	252.24	349.12											
1912	30.04	43.68	78.46	61.28												
2000	36.83	48.09	36.83	48.09												
2006	10.83															
Mean Error	43	75.54	107.33	122.56	149.12	129.62	124.48	138.45	124.42	124.59	110.4	114.27	170.61	169.84	227.04	281.17

Table 3: Cross track error of SAC-Lagrangian advection track prediction model for TC AMPHANw.r.t JTWC real-time observed track

FCST Initial time	Track Error (km) in different Forecast Lead time															
	6	**12**	**18**	**24**	**30**	**36**	**42**	**48**	**54**	**60**	**66**	**72**	**78**	**84**	**90**	**96**
1600	23.18	63.11	60.3	33.39	0	57.22	28.44	76.01	103.9	46.06	35.86	49.78	38.29	74.91	164.5	195.67
1606	0.35	4.58	25.25	0	68.38	87.06	114.59	153.88	11.49	68	76.11	34.76	53.66	118.52	209.13	243.67
1612	13.98	13.22	0	2.37	50.94	69.01	113.28	76.49	22.16	60.51	62.99	44.05	14.24	97.75	153.88	210.81
1700	0	5.19	9.93	41.02	64.3	40.86	92.28	101.35	100.06	79.38	28.26	52.47	62.7	55.9		
1706	30.18	29.03	24.51	13.21	17.95	33.65	55.76	50.85	35.55	41.36	23.16	28.51	23.49			
1712	9.62	31.04	72.75	25.61	19.15	45.65	12.65	3.31	14.57	71.15	59.66	33.13				
1800	29.51	10.04	77.26	106.71	120.61	77.11	30.66	3.22	18.95	54.47						
1806	13.66	31.57	51.15	63.85	77.87	57.34	60.83	46	28.35							
1812	52.31	95.42	157.02	126.63	85.5	41.06	11.57	10.73								
1900	5.03	40.52	107.21	119.29	93.19	92.04										
1906	49.34	99.89	162.92	154.35	136.54											
1912	4.42	30.72	55.92	52.5												
2000	7.6	5.53														
2006	4.34															
Mean Error	17.39	35.37	67.02	61.58	66.77	60.1	57.78	57.98	41.88	60.13	47.67	40.45	38.48	86.77	175.84	216.72

Table 4: Along track error of SAC-Lagrangian advection track prediction model for TC AMPHAN w.r.t JTWC real-time observed track

FCST Initial time	**Track Error (km) in different Forecast Lead time**															
	6	**12**	**18**	**24**	**30**	**36**	**42**	**48**	**54**	**60**	**66**	**72**	**78**	**84**	**90**	**96**
1600	48.5	2.08	6.38	52.52	119.92	147.33	166.6	189.49	163.05	174.89	102.18	82.14	38.05	17.94	13.68	72.02
1606	44.58	77.9	85.91	75.18	48.84	12.31	52.52	95.68	160.58	107.5	2.14	42.22	92.93	109.62	49.47	55.06
1612	67.48	93.76	109.97	122.43	116.48	61.08	30.02	92.48	65.69	19.07	36.18	79.88	148.33	181.61	258.86	322.37
1700	14.13	1.97	13.91	45.58	49.46	89.93	37.44	19.69	77.4	138.91	156.96	159.11	192.44	227.87		
1706	39.58	60.78	47.67	29.85	20.49	30.76	80.02	99.64	140.86	147.99	174.68	236.99	339.52			
1712	10.71	1.05	9.7	81.56	90.34	83.75	83.62	90.23	109.82	94.56	35.91	17.37				
1800	13.55	26.48	31.11	48.03	60.9	68.29	38.33	16.97	21.37	41.75						
1806	66.3	105.67	135	143.38	143.27	108.87	86.64	116.43	158.1							
1812	88.68	170.82	209.88	296.68	332.23	296.97	271.2	292.63								
1900	25.16	103.68	60.48	21.91	72.7	168.96										
1906	7.62	31.73	102.35	199.51	321.31											
1912	29.71	31.06	55.04	31.61												
2000	36.03	47.77														
2006	9.92															
Mean Error	35.85	58.06	72.28	95.69	125.08	106.83	94.04	112.58	112.11	103.52	84.67	102.95	162.25	134.26	107.34	149.82

Table 5: **Direct position error of SAC-Lagrangian advection track prediction model for TC FANI w.r.t IMD Best Track**

FCST Initial time	Track Error (km) in different Forecast Lead time															
	6	**12**	**18**	**24**	**30**	**36**	**42**	**48**	**54**	**60**	**66**	**72**	**78**	**84**	**90**	**96**
2700	62.01	111.45	159.78	210.91	210.68	246.63	278.94	302.46	318.84	296.49	254.03	206.97	161.65	128.09	67.75	44.93
2706	35.42	56.95	69.59	73.44	136.20	154.58	170.56	158.08	144.66	131.59	124.70	121.47	126.01	173.80	217.46	247.53
2712	43.03	47.19	46.45	121.55	95.30	65.42	76.40	103.55	121.71	121.48	163.80	222.61	219.11	167.86	73.64	42.87
2718	39.63	26.16	69.11	63.89	66.05	80.46	76.47	76.30	61.55	129.08	174.61	162.21	99.17	33.66	96.68	169.36
2800	53.81	83.02	84.95	53.21	32.29	56.68	52.58	63.35	79.07	108.28	75.75	18.95	87.94	226.84	315.79	412.45
2806	50.17	62.26	54.26	23.45	36.81	23.02	12.28	52.68	61.31	87.43	122.43	173.17	289.79	355.84	402.50	438.14
2812	16.38	45.72	103.12	130.96	149.01	160.58	185.64	232.83	226.71	169.10	102.55	109.94	190.65	324.55	458.34	547.36
2818	35.67	66.54	81.69	112.11	141.35	209.40	271.51	264.18	208.26	139.74	91.47	187.07	294.03	447.78	543.57	591.00
2900	46.09	64.99	84.95	97.88	121.52	169.03	169.29	117.47	28.13	117.79	208.12	314.20	435.48	455.36	475.17	519.24
2906	17.33	20.04	42.05	53.62	88.64	80.60	39.10	70.27	129.37	149.83	179.49	237.40	235.11	250.68	251.48	240.90
2912	18.13	25.67	54.75	91.06	72.58	40.80	26.70	89.72	99.86	136.08	189.13	193.94	198.46	226.91	193.16	
2918	29.42	63.88	95.59	91.72	73.44	46.47	61.14	34.75	20.76	73.21	88.99	76.64	102.50	98.49		
3000	43.47	84.93	88.59	59.41	56.86	41.77	49.05	89.29	140.06	139.68	104.66	52.02	21.69			
3006	39.20	75.94	48.06	39.57	30.50	35.30	84.07	149.78	160.47	183.44	222.07	182.94				
3012	29.28	23.25	30.78	99.44	147.83	193.49	210.99	169.65	117.21	137.54	125.94					
3018	45.15	33.41	42.53	9.88	30.10	72.42	101.36	103.57	135.62	116.92						
0100	16.71	45.47	34.54	65.64	76.87	46.70	26.71	91.82	95.66							
0106	42.92	47.38	30.50	52.04	60.07	41.07	70.18	133.76								
0112	27.02	50.09	71.15	57.92	71.46	112.57	108.72									
0118	17.38	18.24	11.90	86.73	122.93	163.43										
0200	33.97	24.13	17.84	57.02	98.65											
0206	18.86	7.00	29.50	42.45												
0212	12.31	20.46	55.64													
0218	15.31	33.62														
Mean Error	**32.86**	**47.41**	**61.19**	**77**	**91.39**	**102.02**	**109.04**	**127.97**	**126.43**	**139.86**	**148.52**	**161.39**	**189.35**	**240.82**	**281.41**	**325.38**

IMD reported that cyclone AMPHAN crossed West Bengal – Bangladesh coasts as a very severe cyclonic storm across Sundarbans, near lat.21.65°N/long. 88.3°E during1000-1200 UTC on 20 May 2020, with maximum sustained wind speed of 85 knots gusting to 100 knots.

The landfall point and time error of all the real-time generate track forecasts by SAC-model has been computed with respect to IMD estimated landfall position and have been summarized in the Table 6.

Table 6: Land-fall point error (km) of SAC-Lagrangian advection track prediction model for TC AMPHAN

Forecast initial time	Landfall point		Landfall time	Landfall Error	
	Longitude	Latitude		Position Error (km)	Time Error (hours)
200516 00Z					
200516 06Z					
200516 12Z					
200517 00Z	88.51	21.83	20 May 18 Z	29.51	+7 hours
200517 06Z	88.12	21.90	21 May 04 Z	33.44	+17 hours
200517 12Z	87.24	21.54	20 May 10 Z	53.92	-1 hours
200518 00Z	88.51	21.54	20 May 09 Z	24.92	-1 hour
200518 06Z	88.04	21.55	20 May 15 Z	29.09	+4 hours
200519 00Z	87.84	21.73	20 May 17 Z	48.35	+6 hours
200519 06Z	88.24	21.58	21 May 02 Z	9.95	+15 hours
200519 12Z	87.68	21.65	20 May 19 Z	64.08	+8 hours
200520 00Z	88.12	21.62	20 May 09 Z	18.90	-2 hours
200520 06Z	88.14	21.63	20 May 10 Z	16.69	-1 hours

It can be seen that landfall error, of track predicted within 24 hours (00 UTC 20 MAY 2020), in position was 18 km and time was two hours advance.

The forecasts from SAC model can be further improved by including the high resolution (17 km x 17 km) first guess conditions provided by NCMUM model from National Centre of Medium Range Weather Forecast (NCMRWF) in place of currently being used 50 km x 50 km gfs initial conditions.

3.3 Intensity Prediction of TC AMPHAN

Intensity of TC AMPHAN was predicted using output of HWRF model which is operationally run at NCEP. Real-time generated intensity product is shown in the figure.

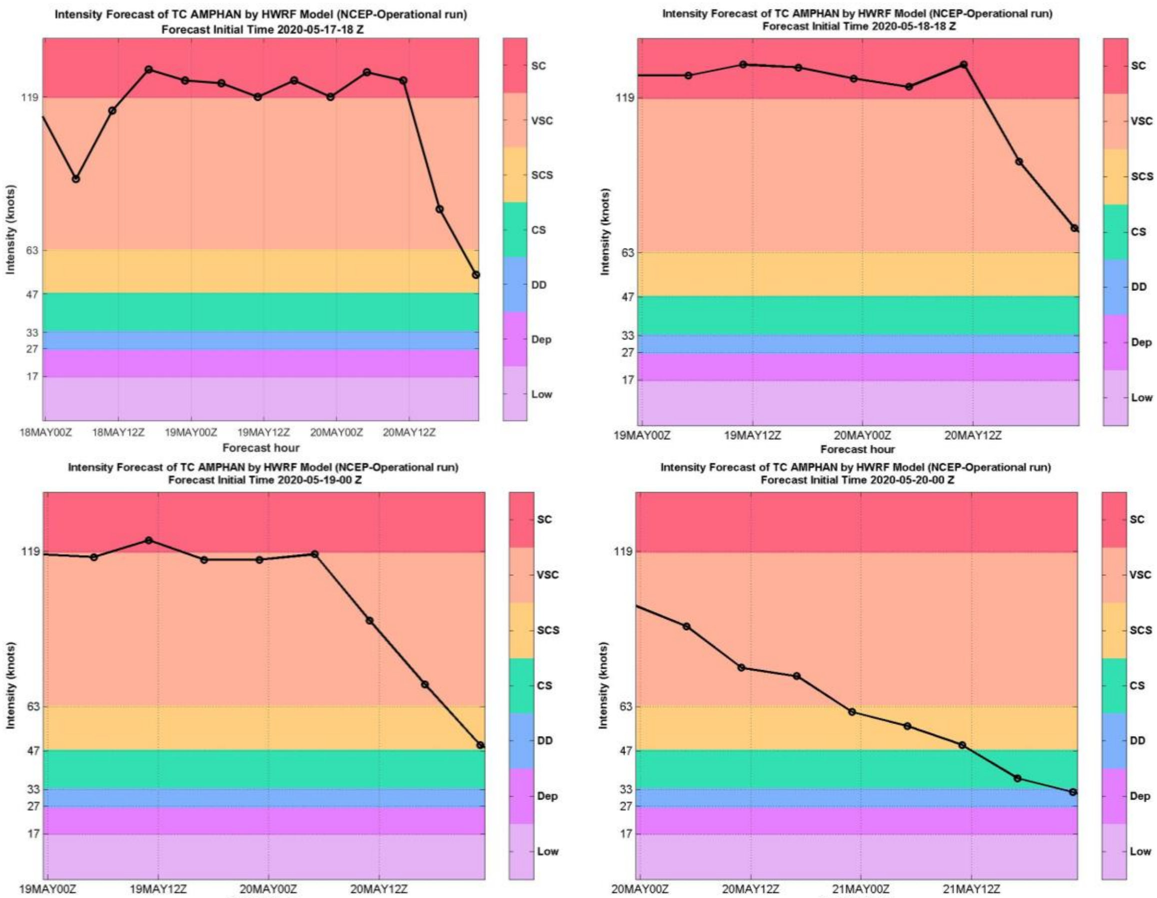

Figure 5: Real-time generated intensity prediction of TC AMPHAN during 00 UTC of 17- 20 May, 2020.

3.4 Ship Avoidance Region Prediction for TC AMPHAN

For vessels at sea, avoiding the 34 knot wind field of a tropical cyclone is paramount. Any ship in the vicinity of a tropical cyclone should make every effort to remain clear of the maximum radius of analyzed or forecast 34 knot winds associated with the tropical cyclone. Knowing that the area of 34 knot around tropical cyclones is rarely symmetric but instead varies within semi-circles or quadrants is important. Understanding that each tropical storm or hurricane has it own unique 34 knot wind field are necessary factors to account for when attempting to remain clear of this dangerous area around a tropical cyclone. Based on operational HWRF 34 knot wind radial distances the graphical inputs of ship avoidance region was also generated for TC AMPHAN and disseminated through SCORPIO server.

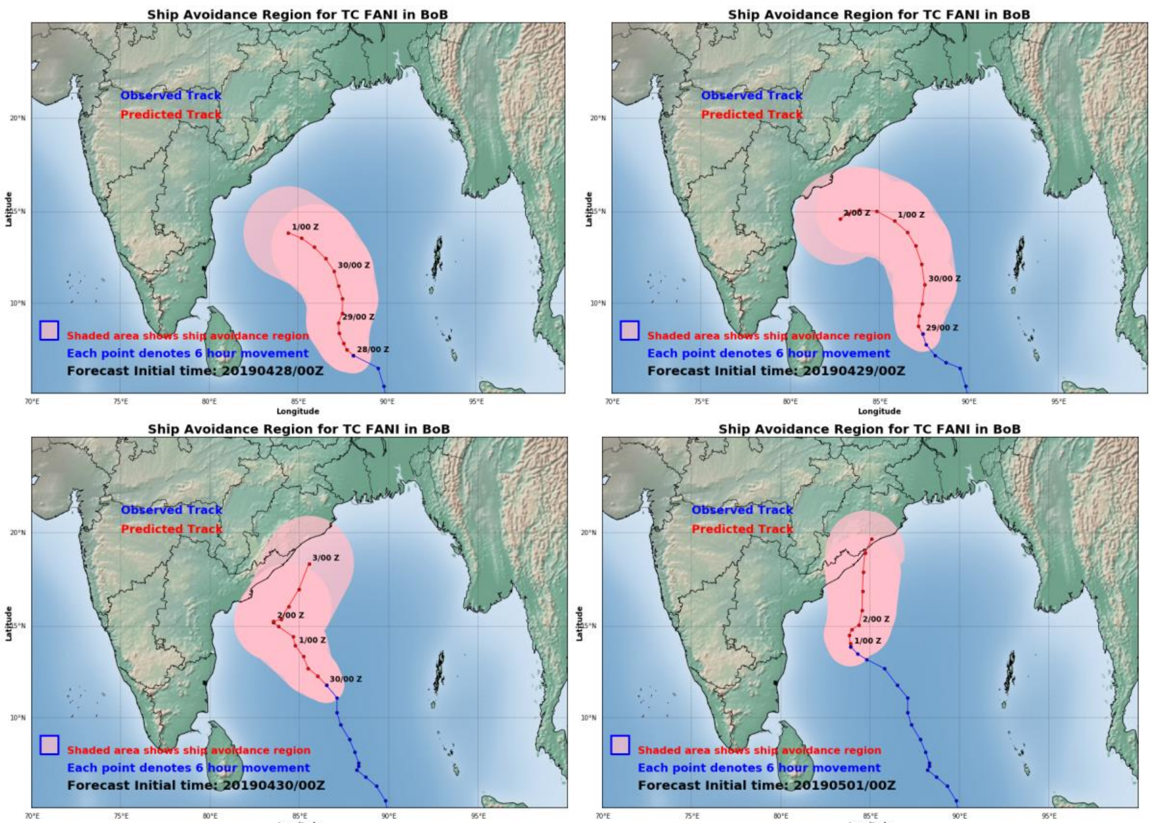

Figure 6: Real-time predicted ship avoidance region for TC AMPHAN during 00 UTC of 16- 20 May, 2020.

4. Satellite Observations over TC AMPHAN

Different sensors onboard the geostationary and polar orbiting satellites provide observations at different times and different phases of intensification of TCs which are very useful to estimate the correct geo-location of the system and retrieve its structural parameters. Different satellite observations over TC AMPHAN have been discussed in this section.

4.1 INSAT 3D Products

Cyclone Geo-location

TC AMPHAN was continuously observed by the half hourly acquisition of INSAT-3D satellite. In half hourly TIR imageries of INSAT 3D satellite the center location of cyclone was estimated by center determination algorithm developed at SAC. The results were disseminated through SCORPIO web-server. One of the sample products generated in the real-time has been shown in the Fig. 7.

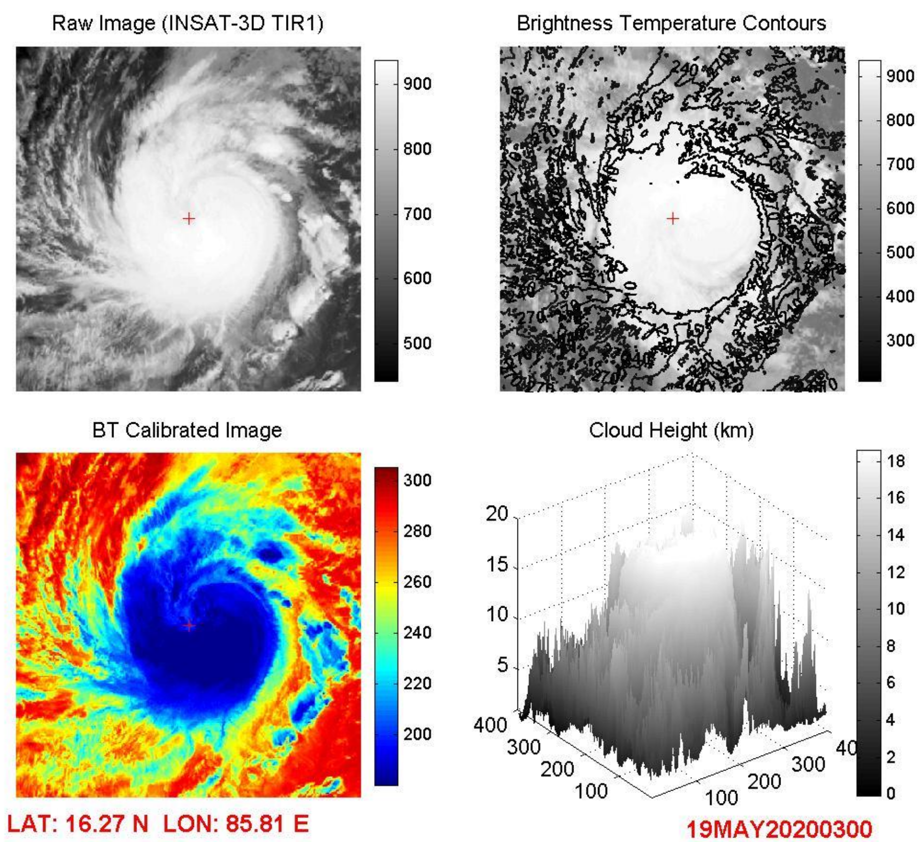

Figure 7: Center of TC estimated using INSAT 3D TIR image (0300Z 19 May, 2020).

Cyclone centric products of INSAT3D satellite

A procedure has been developed to produce cyclone centric products from each half hourly image of INSAT3D satellite. These images are very useful to study the structural changes in the core of tropical cyclone. A sample product generated on 0300 Z 19 May, 2020 have been presented in the Figure 8.

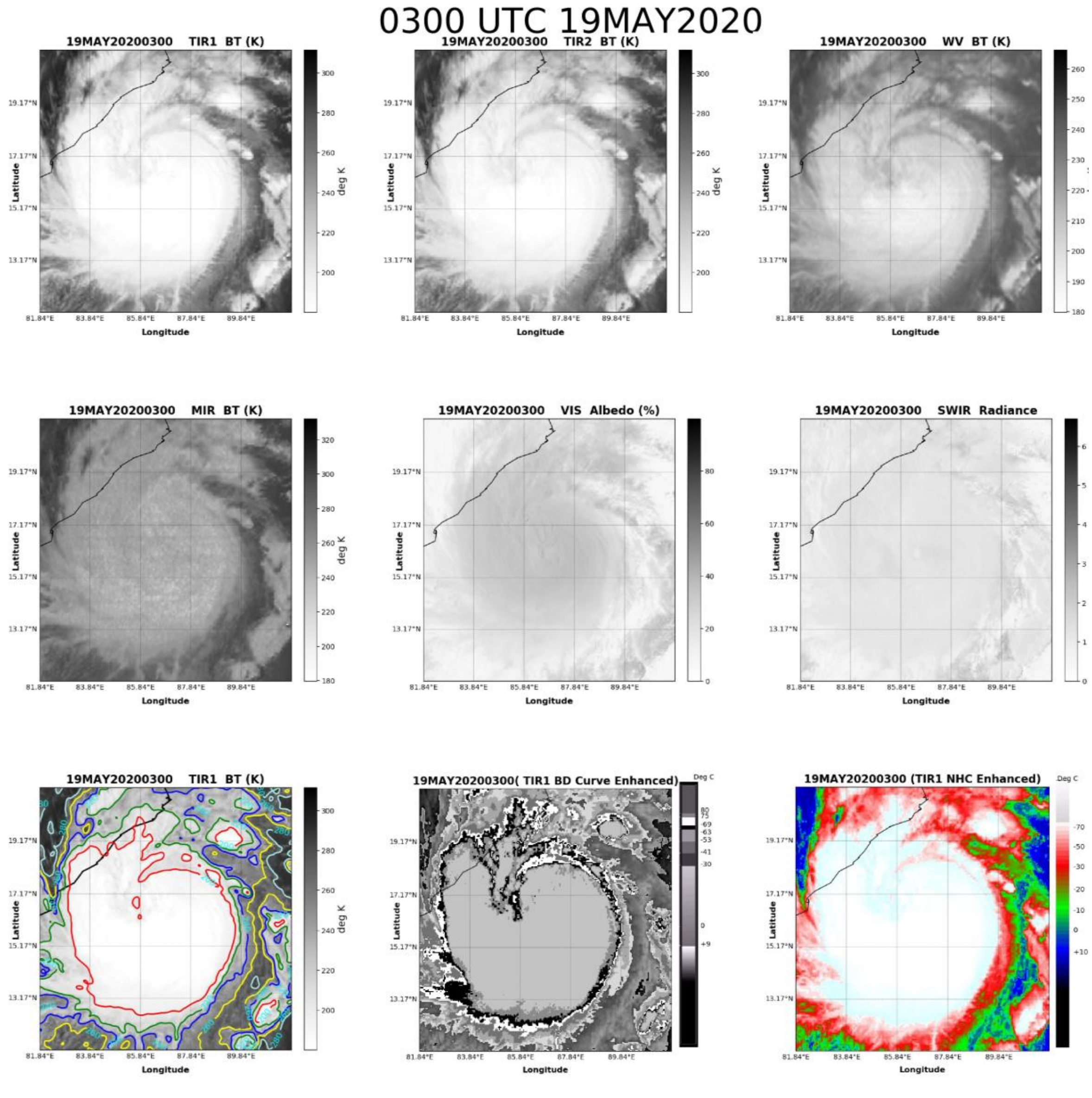

Figure 8: Cyclone centric products of INSAT3D imager channels

4.2 INSAT-3DR rapid scan observations over TC AMPHAN

High spatial and temporal resolution images from geo-stationary satellites are the primary tool for real-time monitoring and intensity analysis of Tropical Cyclones (TCs). Weather events over the Indian region are continuously monitored by two Indian geostationary satellites i.e. INSAT-3D and INSAT-3DR at a frequency of 15 minutes in staggered mode. During extreme weather events like TCs, INSAT-3DR is operated in rapid scan operation mode by taking observations over the system at 4-minute intervals. These observations are highly useful in understanding the instantaneous structural changes during evolution, intensification and landfall of TCs. The salient observations over the cloud systems by visible, thermal infrared (TIR1), and water vapour (WV) imageries from INSAT-3DR during the life cycle of TC AMPHAN were obtained during TC AMPHAN. Few images during intensification stage of TC AMPHAN on 18 May 2020 from TIR-1 and visible channels are shown in the Figure 9 and 10, respectively.

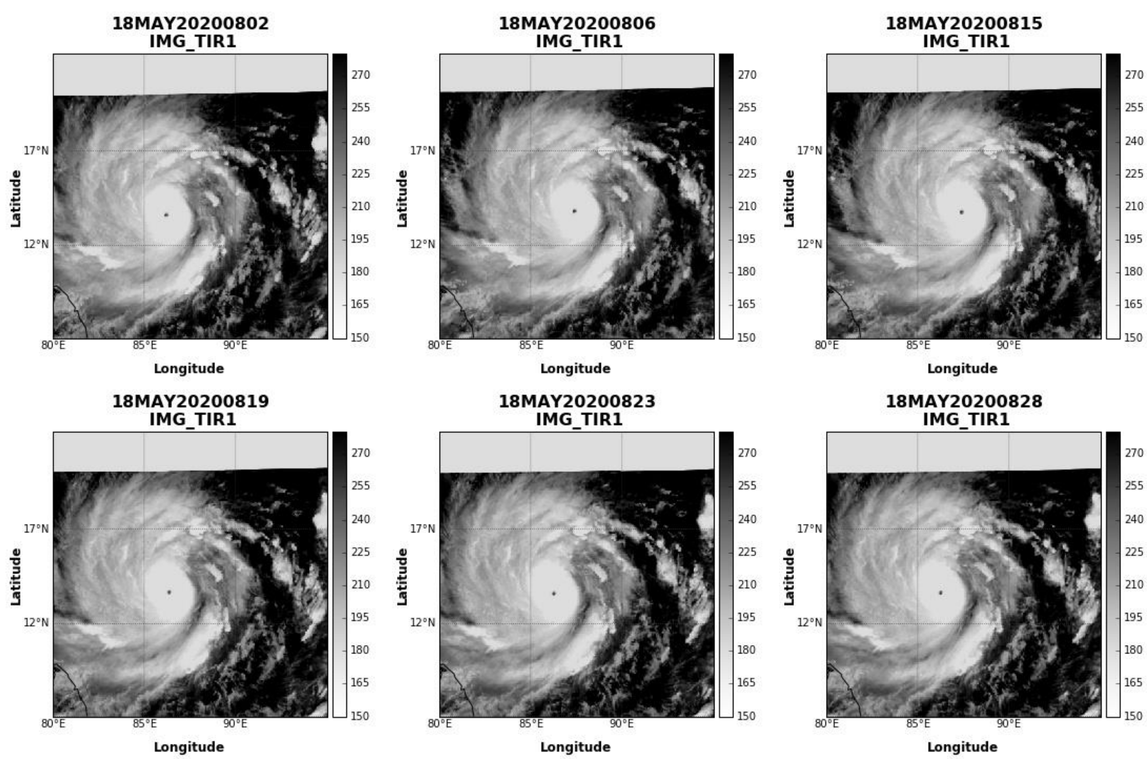

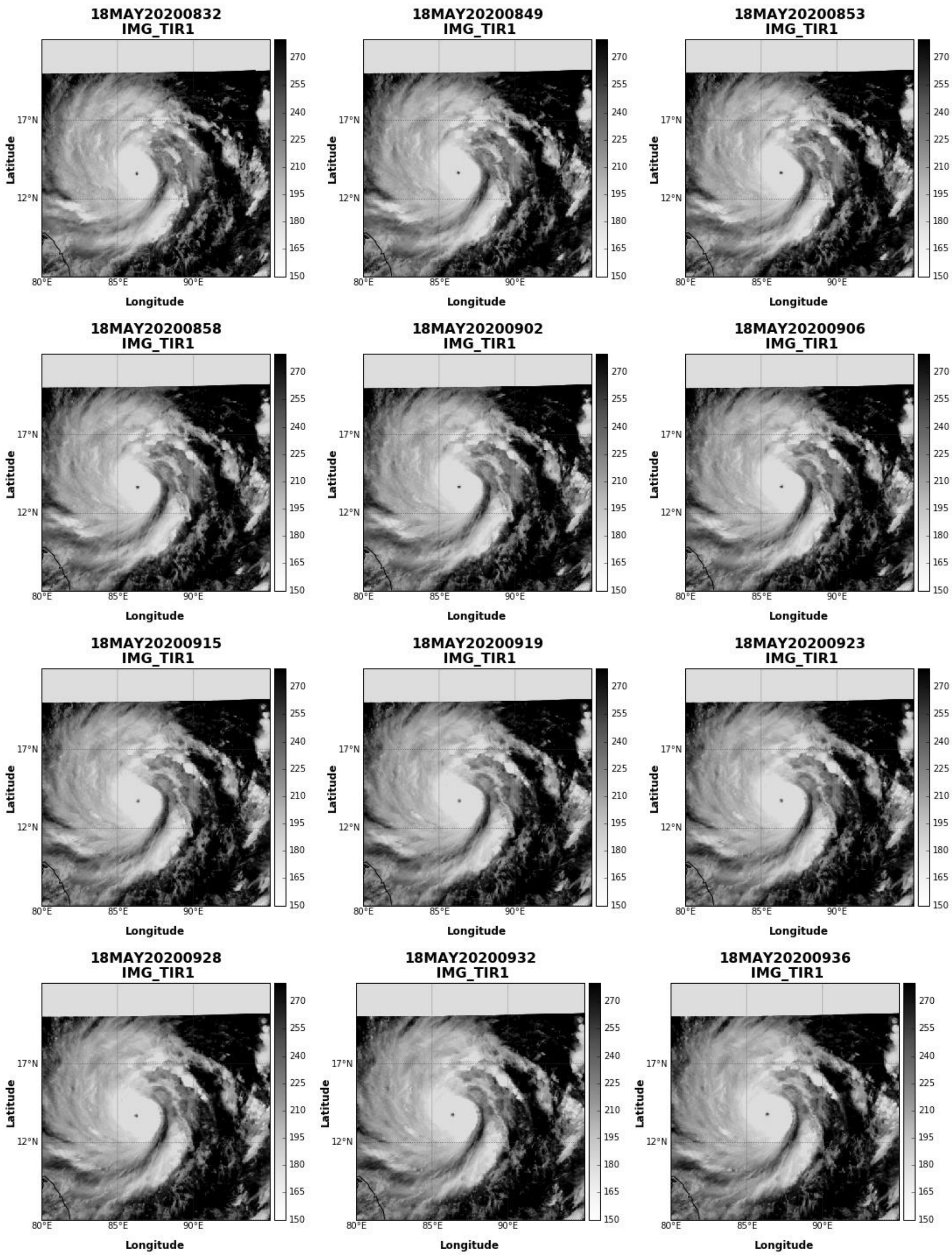

Figure 9: INSAT-3DR generated rapid scan images over TC AMPHAN during 0802 UTC-0936 UTC 18 May 2020 from TIR-1 channel.

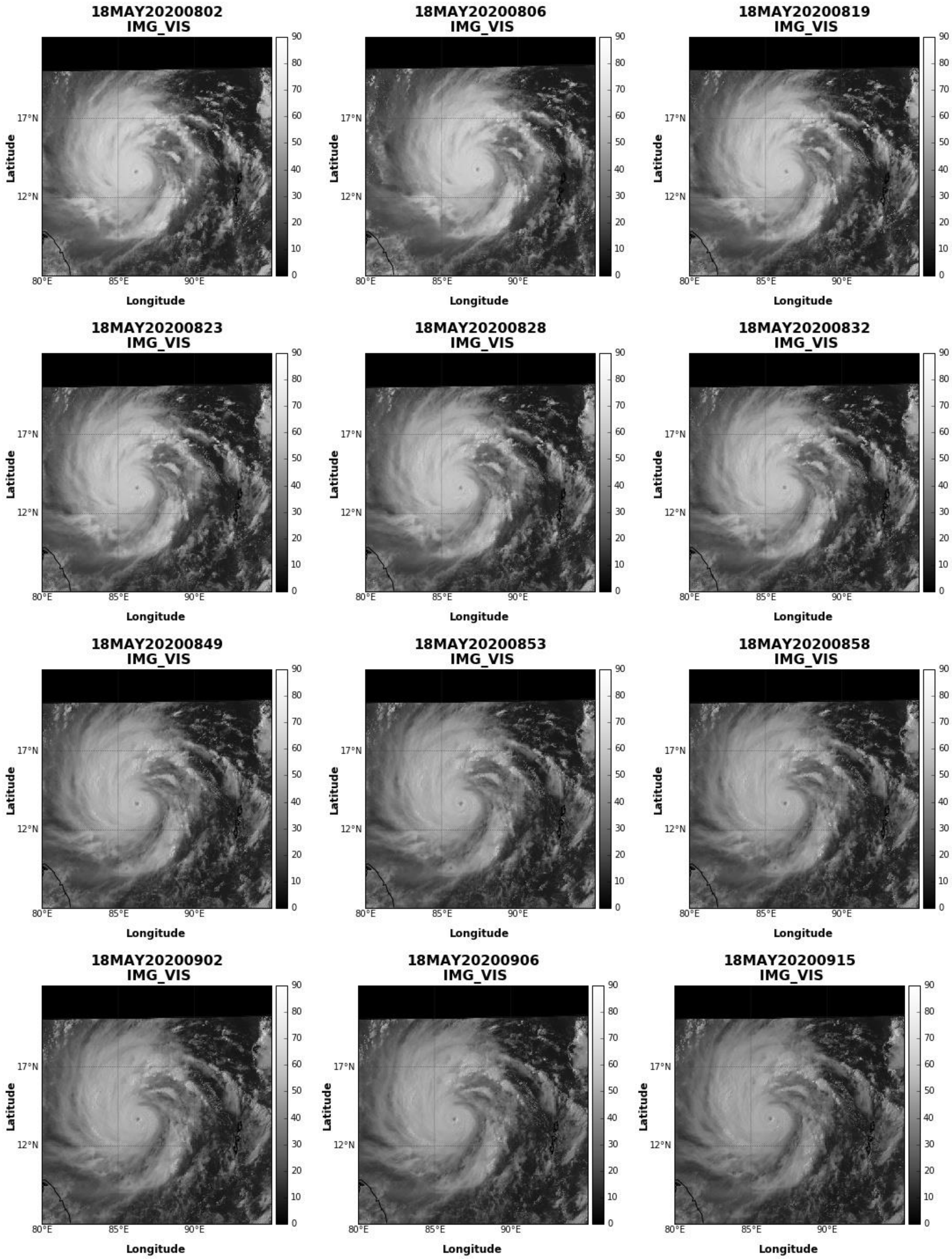

Figure 10: INSAT-3DR generated rapid scan images over TC AMPHAN during 0802 UTC-0936 UTC 18 May 2020 from visible channel.

4.3 Satellite based surface wind observations over TC AMPHAN

The wind observations over TC AMPHAN observed by different sensors onboard different Indian and foreign satellites e.g. SCTASAT-1, CYGNSS, SMAP and WINDSAT have been discussed in this section.

4.3.1 SCATSAT-1

The SCATSAT-1 satellite had six coverage over cyclone AMPHAN during its life over ocean. The wind vectors (L2B: 25 km x 25 km) from all the pass covering the cyclonic have been shown in the Figure 11. The observations of surface wind vectors over TC AMPHAN by SCATSAT-1 have been analyzed. The maximum wind speed captured by the SCATSAT passes have been shown in the Figure 16 along with JTWC maximum sustained wind speed. The JTWC wind speed are converted into 10 minute averaged wind by multiplying the factor 0.9. The satellite estimates are equivalent to 10 minute average wind speed values. Four SCATSAT passes shows the full coverage over the system however, three passes captured the partial coverage and 20th May (evening) shows the system close to land.

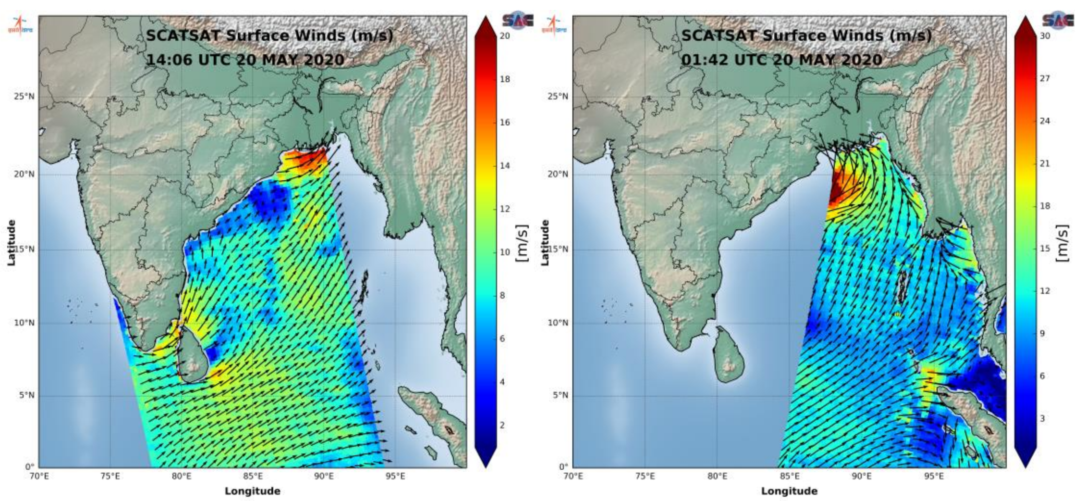

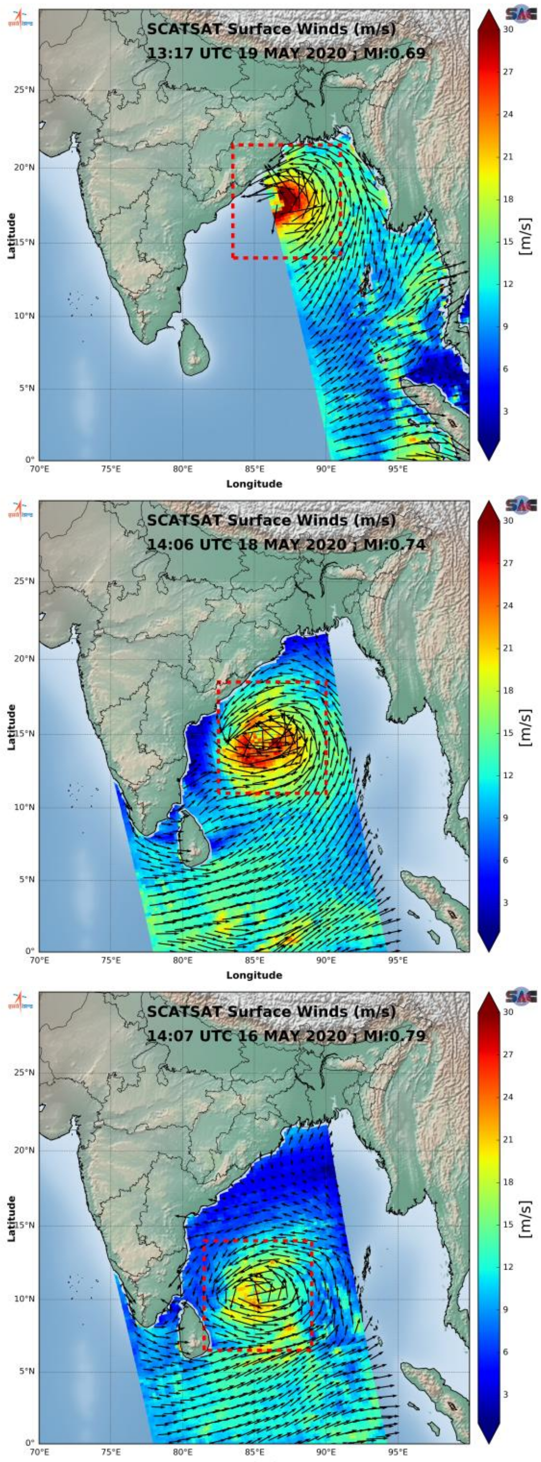

Figure 11: SCATSAT-1 wind vector products over the TC AMPHAN (16th -20th May, 2020)

4.3.2 CYGNSS

CYGNSS (Cyclone Global Navigation Satellite System) is part of the NASA ESSP (Earth System Science Pathfinder) program referred to as an EVM (Earth Venture Mission). CYGNSS will use a constellation of eight small satellites in LEO (Low Earth Orbit) carried to orbit on a single launch vehicle. In orbit, CYGNSS's eight microsatellite observatories will receive both direct and reflected signals from GPS (Global Positioning System) satellites. The direct signals pinpoint CYGNSS observatory positions, while the reflected signals respond to ocean surface roughness, from which wind speed is retrieved.

The overall objective of CYGNSS is to improve extreme weather predictions. The mission is focused on tropical cyclone (TC) inner core process studies. CYGNSS attempts to resolve the principle deficiencies with current TC intensity forecasts, which lie in inadequate observations and modeling of the inner core. The inadequacy in observations results from two causes viz. (i) much of the inner core ocean surface is obscured from conventional remote sensing instruments by intense precipitation in the eye wall and inner rain bands and (ii) the rapidly evolving (genesis and intensification) stages of the TC life cycle are poorly sampled in time by conventional polar-orbiting, wide-swath surface wind imagers. CYGNSS is specifically designed to address these two limitations by combining the all-weather performance of GNSS bistatic ocean surface scatterometry with the sampling properties of a constellation of eight satellites. The use of a dense constellation of microsatellites results in spatial and temporal sampling properties that are markedly different from conventional imagers.

The observations by the constellations of CYGNSS system over TC AMPHAN have been obtained from the podaac website "https://podaac-tools.jpl.nasa.gov/drive/files/allData/cygnss/L3/v2.1" and is shown in the Figure 12. All the passes within a day have been plotted together. The maximum wind speed observed by the satellite system has been summarized in the Fig. 16.

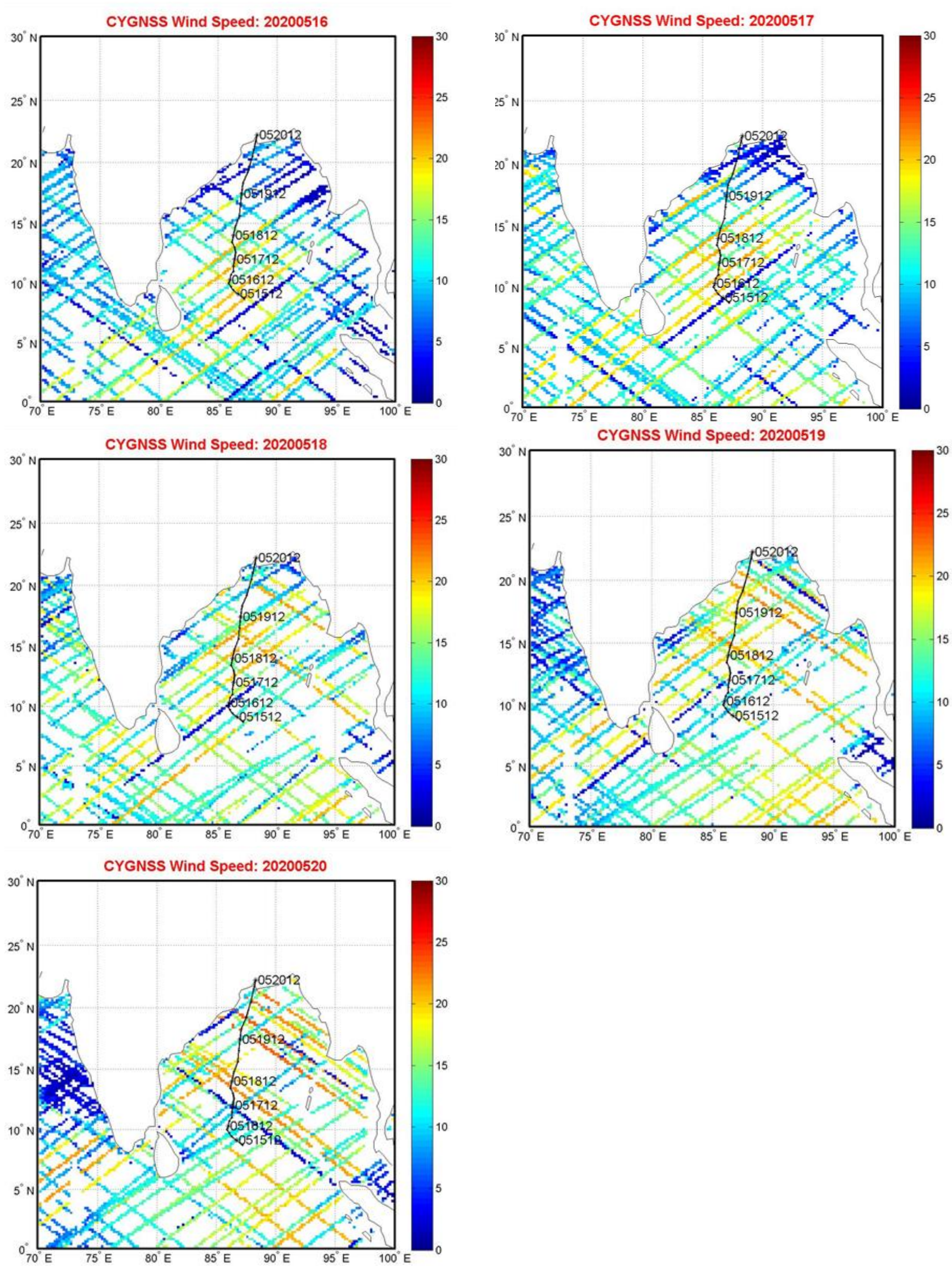

Figure 12: CYGNSS wind speed products over the TC AMPHAN (16 -20 May, 2020).

4.3.3 SMAP

Soil Moisture Active Passive (SMAP) is a United States environmental research satellite launched on 31 January 2015. The SMAP observatory includes a dedicated spacecraft and instrument suite in a near-polar, Sun-synchronous orbit. The SMAP measurement system consists of a radiometer (passive) instrument and a synthetic aperture radar (active) instrument operating with multiple polarizations in the L-band range. The combined active and passive measurement approach takes advantage of the spatial resolution of the radar and the sensing accuracy of the radiometer.

SMAP provides two wind speed products e.g. (i) Near-Real Time (NRT) wind speed and (ii) Final wind speed product. The NRT wind processing uses ancillary fields of shorter latency but lower quality. A Final Wind Speed version, reprocessed with a 1-month delay, which uses higher quality ancillary data. The wind speed from NRT product of SMAP over TC AMPHAN were obtained from the remote sensing system ftp site (ftp://ftp.remss.com/smap/wind/L3/v01.0/daily/NRT/2020/) and has been shown in the Fig. 13. There were three passes of SMAP over the TC AMPHAN during its different intensity stages.

Additionally, SMAP also provide Tropical Cyclones (TC) ASCII files with SMAP 10-min maximum-sustained winds (in kn) and wind radii (in nm) for the 34 kn (17 m/s), 50 kn (25 m/s), and 64 kn (33 m/s) winds for each SMAP pass over a TC in all tropical ocean basins. The wind radii estimated by SMAP satellite for TC AMPHAN for four of its full coverage pass has been shown in the Figure 14. The values have been summarized in Table 7.

Table 7: Critical wind radii estimates by SMAP product

Pass Time (MMDD)	Maximum Wind (kt)	R34: 34 knots wind radii (nm)				R50: 50 knots wind radii (nm)				R64: 64 knots wind radii (nm)			
202005181215	103	0	0	165	165	75	69	95	105	53	52	55	40
202005190025	113	181	147	157	0	104	92	113	119	66	62	91	90
202005201152	46	0	0	0	0	0	0	0	0	0	0	0	0

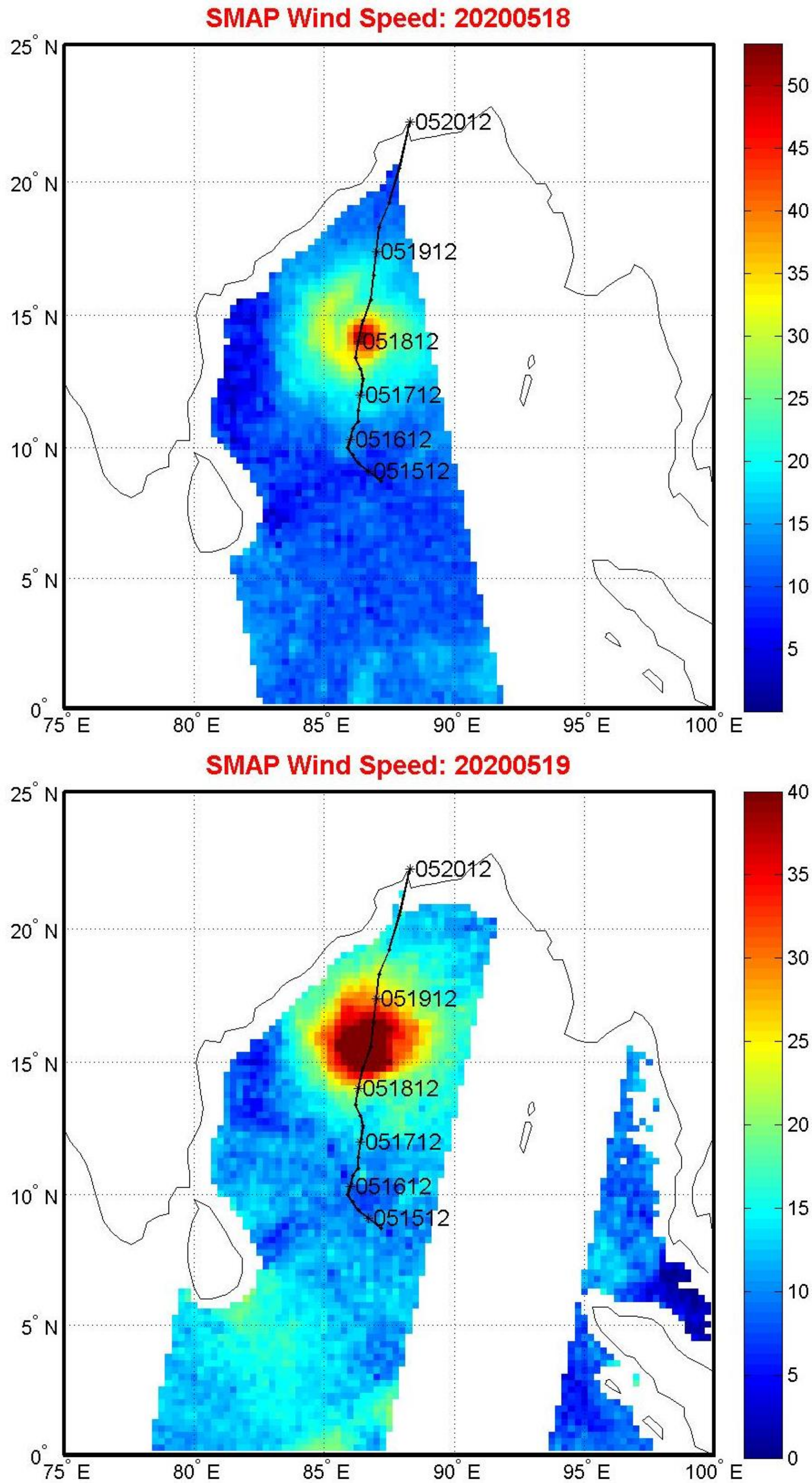

Figure 13: SMAP wind speed NRT products over TC AMPHAN (16 -20 May 2020)

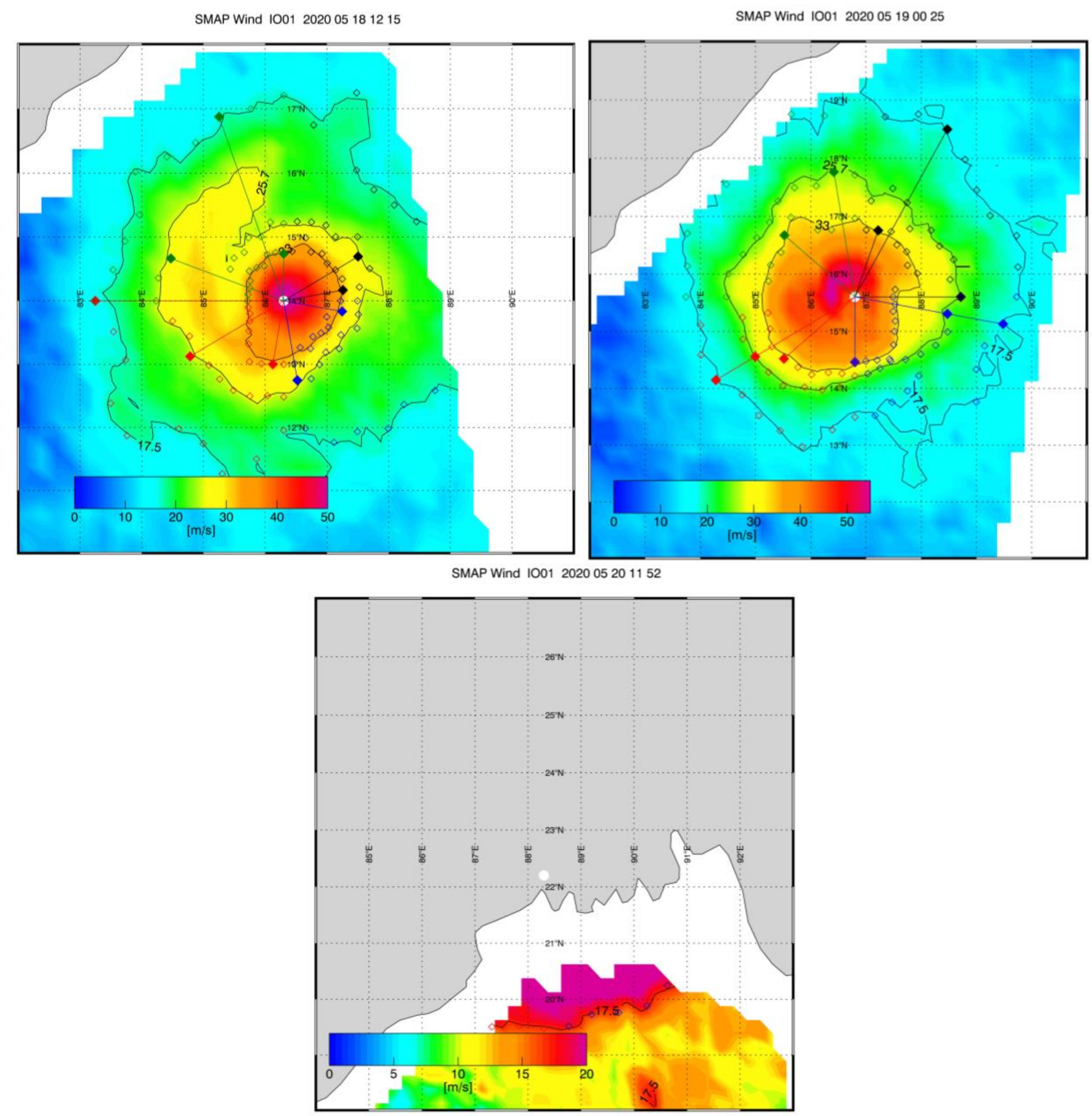

Figure 14: SMAP critical wind radii estimation over TC AMPHAN (SMAP real time products obtained from www.remss.com)

4.3.4 WINDSAT

The WindSat Polarimetric Radiometer was developed by the Naval Research Laboratory (NRL) Remote Sensing Division and the Naval Center for Space Technology for the U.S. Navy and the National Polar-orbiting Operational Environmental Satellite System (NPOESS) Integrated Program Office (IPO). It was launched on January 6, 2003 aboard the Department of Defense Coriolis satellite. WindSat was meant to demonstrate the capabilities of a fully polarimetric radiometer to measure the ocean surface wind vector from space. Prior to launch, the only instrument capable of measuring ocean wind vectors were scatterometers (active microwave sensors). In addition to wind speed and direction, the instrument can also measure sea surface temperature, soil moisture, ice and snow characteristics, water vapor, cloud liquid water, and rain rate.

The near real time (NRT) product of all-weather wind speed, WSPD_AW, over TC AMPHAN have been shown in the Figure 15. The final WSPD_AW product is generated after a month which is a smooth blend between the standard wind speed obtained in non-raining conditions WSPD_LF, the global wind speed through rain and the H-wind derived wind speed.

There were two full and two partial coverage of WINDSAT over TC AMPHAN. The maximum wind speed observed by NRT product in all these passes were analysed and summarized in Figure 16.

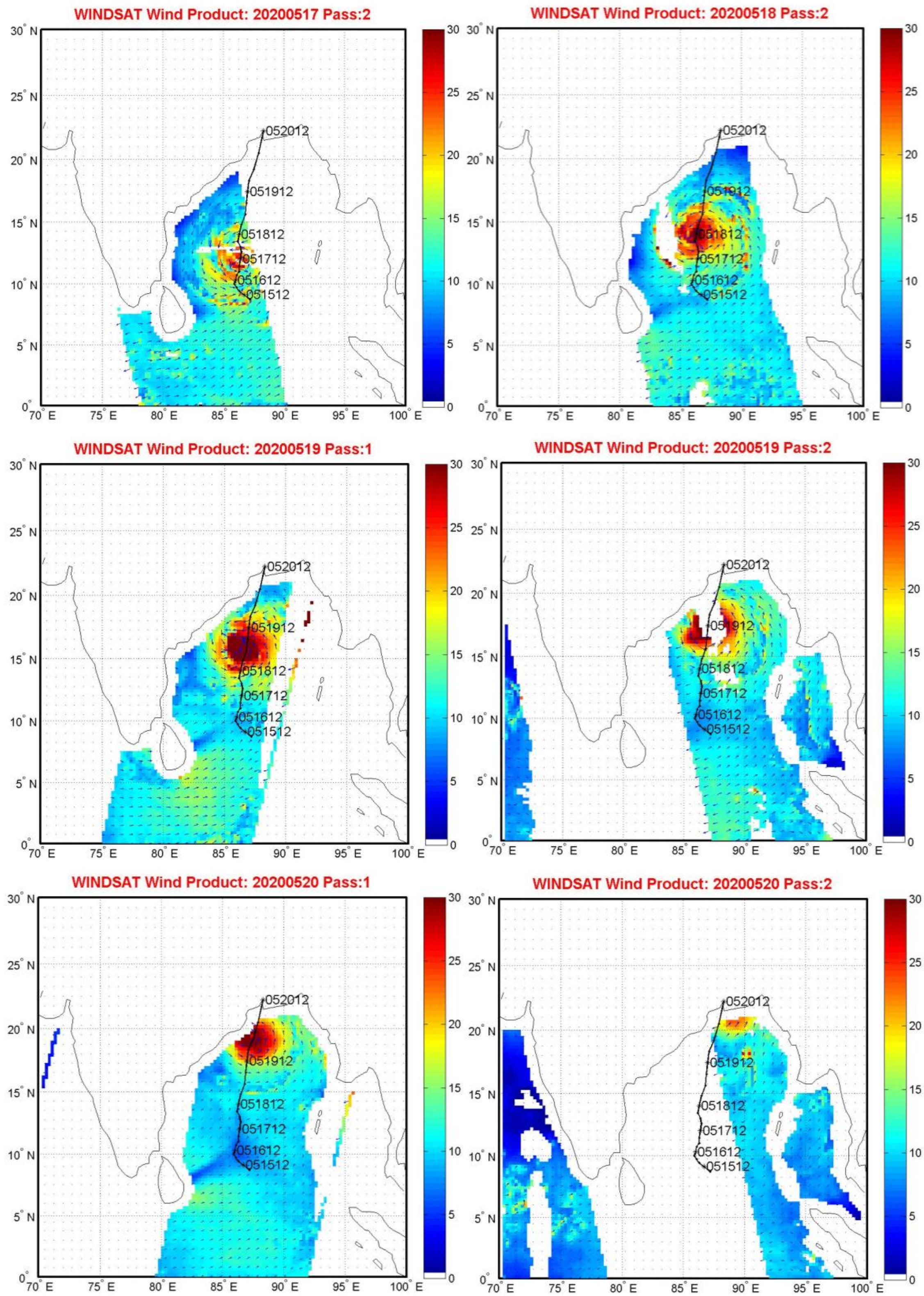

Figure 15: WINDSAT wind vectors NRT products over TC AMPHAN (16 -20 May 2020)

4.3.5 Comparison of Satellite Wind Speed Products

The maximum wind speed estimated in the inner core of the cyclone during its pass over TC AMPHAN by all the above mentioned satellites have been shown in the Figure 16. The JTWC real-time estimated wind speed at every 6-hour interval is also plotted in the figure. The figure shows that SCATSAT-1 gives good estimates of wind speed upto 30 m/s. After that the values are underestimated. This underestimation by SCATSAT for higher winds is due to its obvious reason of backscatter signal contamination during high rain conditions. The values of SMAP were found to be very well estimated with the JTWC observed wind estimates. SMAP has found to be accurately estimating the winds upto nearly 60 m/s. The maximum wind speed estimated by CYGNSS wind product was upto approximately 21 m/s only. The high winds are not found to be captured by CYGNSS wind product. WINDSAT wind speed estimates were also underestimated during very high wind speed conditions i.e. beyond 30 m/s. TC AMPHAN was Super cyclone with wind speed upto 68 m/s. The SMAP satellite wind products have shown their potential to estimate such high wind estimates. The analysis is based on the NRT products which shows that SMAP wind can also be utilized during real-time.

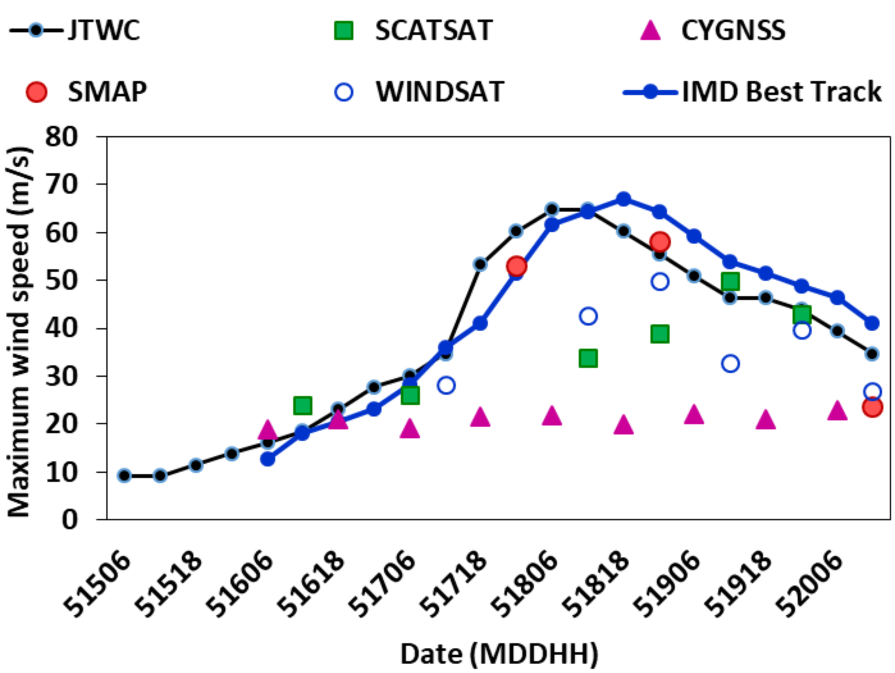

Figure 16: Inter-comparison of maximum wind speed estimated by satellite products over TC AMPHAN

5. Dissemination of Forecasts through web

Satellite Based Cyclone Observation and Real-time Prediction over Indian Ocean (SCORPIO) (https://mosdac.gov.in/scorpio) is a web-based application designed to provide Web-GIS based real-time Cyclone Information services over the North Indian Ocean. SCORPIO is available on the MOSDAC portal (https://mosdac.gov.in). It works as a decision support system to support the Disaster management System. Considering the criticality of timeliness for cyclone warning and prediction, the SCORPIO web-portal has been designed to operate in near total automation. It has module for automatic detection of Cyclogenesis using the Near Real-time SCATSAT Wind data. Alert is generated and updated automatically on SCORPIO site if any cyclogenesis condition is detected over the Indian Ocean.

For the cyclone AMPHAN, the SCORPIO website was updated in real-time with the following information:

- Prediction of cyclogenesis, winds observed by SCATSAT over the north Indian Ocean region,
- Cyclone centric images generated by different channels of INSAT-3D satellite,
- Track prediction by SAC-Lagrangian advection model
- Intensity prediction by NCEPHWRF model
- Ship avoidance region
- Cyclone center using INSAT3D data

The webpage of SCORPIO web-portal during the cyclone AMPHAN has been shown in the Fig.17 -19.

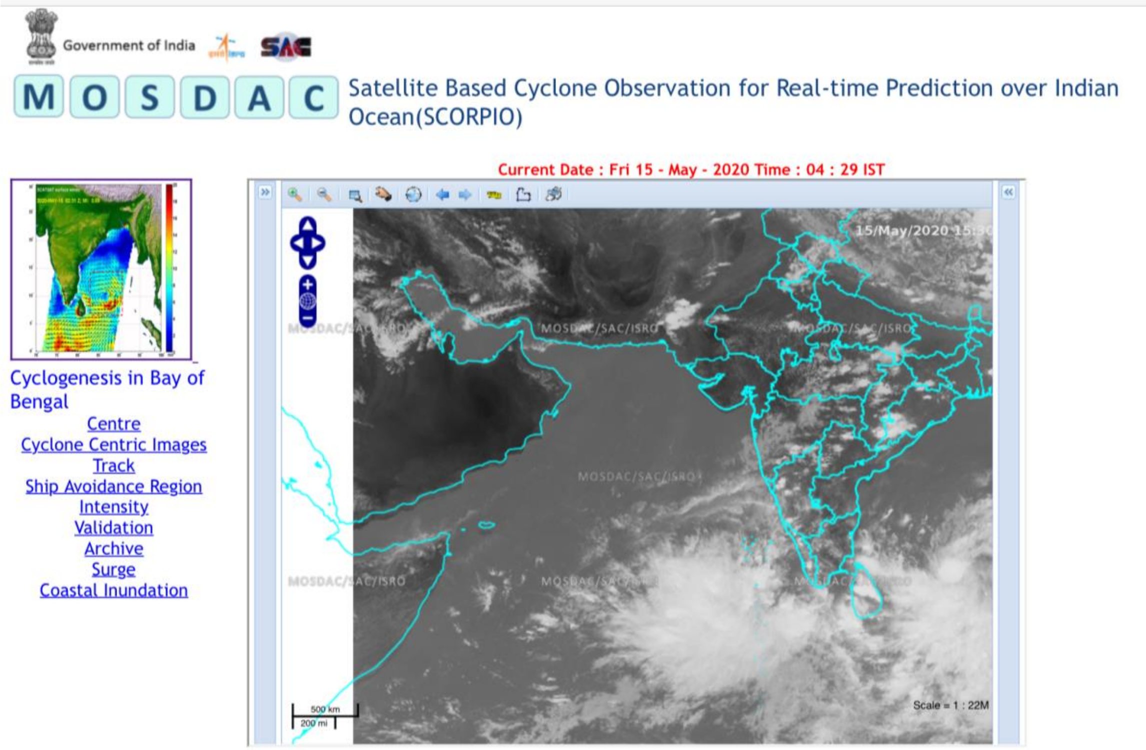

Figure 17: SCORPIO webpage showing the cyclogenesis alert of TC AMPHAN (15 May 2020).

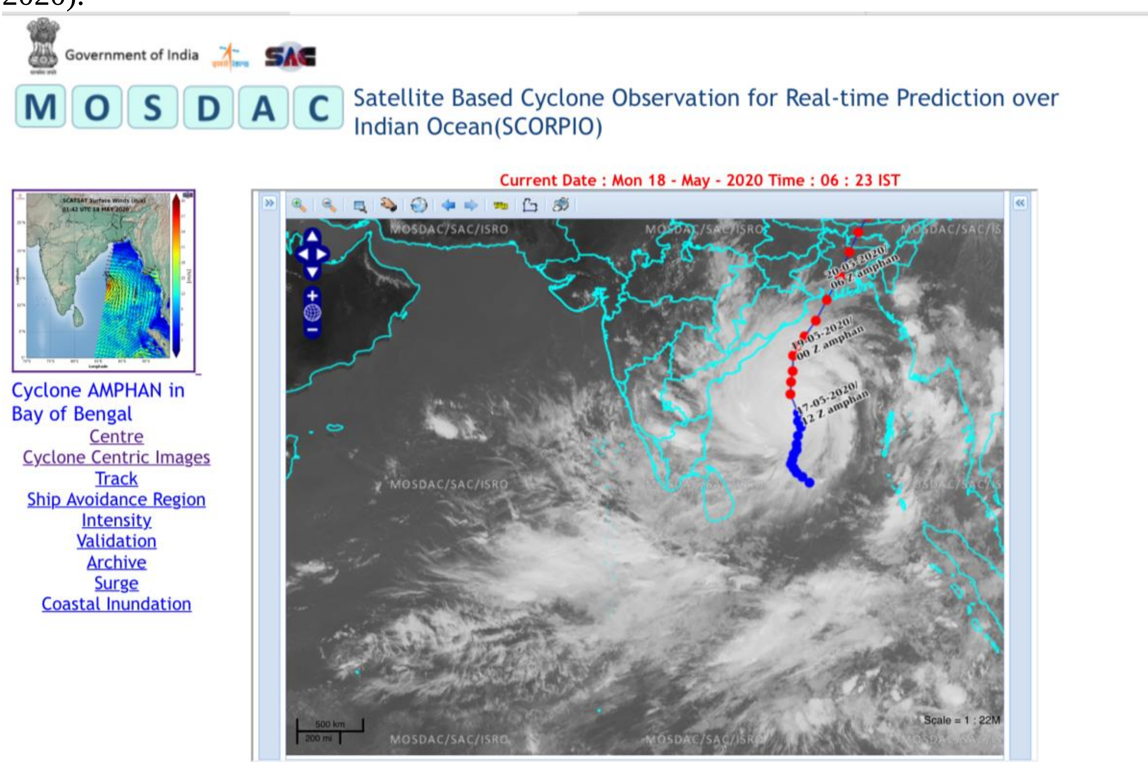

Figure 18: SCORPIO webpage during the active phase of TC AMPHAN (18 May 2020).

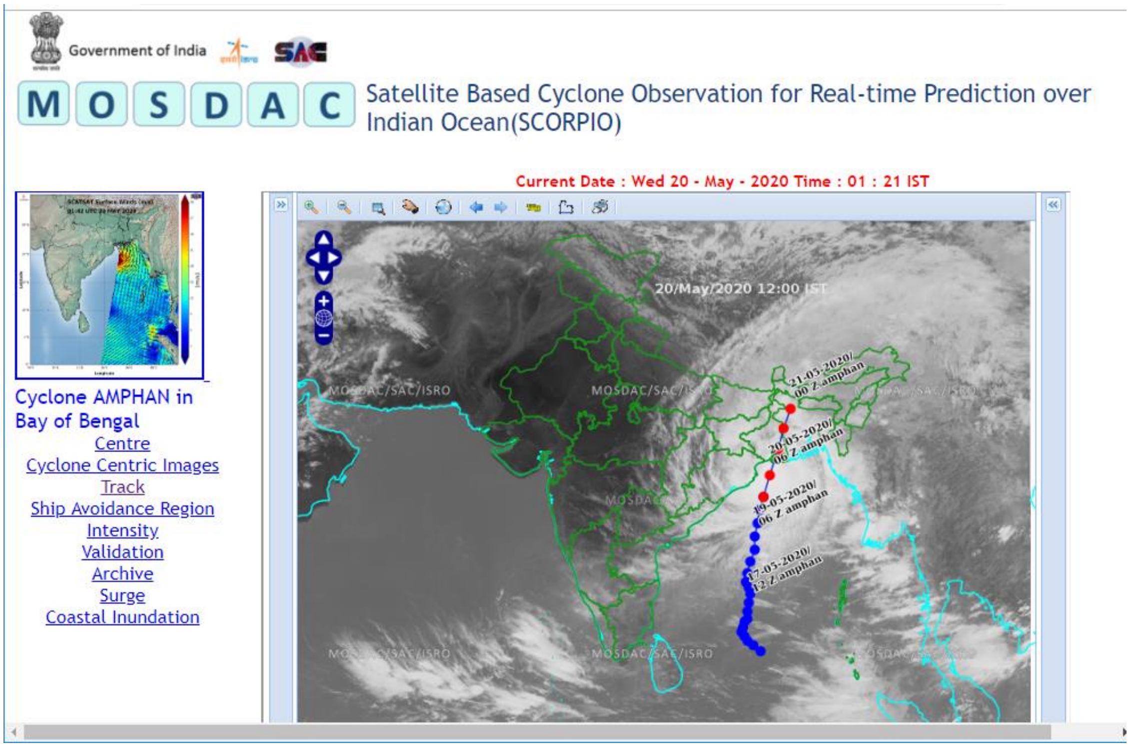

Figure 19: SCORPIO webpage during the landfall of TC AMPHAN (20 May 2020).

6. Conclusions

The real-time monitoring and prediction of TC AMPHAN based on in-house developed techniques and the satellite products have been summarized in this report.

The real-time track prediction of track TC based on in-house developed model SAC-LAGAM for different initial conditions at 00 06 12 and 18 UTC during 16 to 20 May 2020 have been presented in the report. The track error with respect to JTWC observed track has been computed for all forecast lead hours. It has been shown that for TC AMPHAN the mean track error (direct position error) for lead prediction time 24, 48, 72 and 96 hours was 123 km, 138 km, 114 km and 281 km, respectively. It can be seen that landfall error, of track predicted within 24 hours (00 UTC 20 MAY 2020), in position was 18 km and time was two hours advance.

Scatsat-1 did not capture the cyclone during its genesis stage. The cyclogenesis of TC AMPHAN was predicted as a developing system on 02 UTC 14 May 2020 using the SCATSAT wind data as the wind pattern matching index values at the vortex were exceeding the predetermined threshold of 0.6. The cyclogenesis alert was disseminated through SCORPIO web-portal of MOSDAC (Meteorological and Oceanographic Satellite Data Archive Centre) and also communicated to cyclone warning division at India Meteorological Department (IMD), New Delhi

The real-time satellite cyclone centric products from Indian satellite INSAT-3D and SCATSAT-1 were generated in the real-time and has been discussed in this report. The real-time products of TC intensity forecast and ship avoidance region prediction based on the NCEP-operational hurricane-WRF model were provided in the real-time and are presented in this report.

The wind speed estimated by different satellite products (available in near real-time) have been presented in this report for all passes of satellites (SCATSAT-1, CYGNSS, SMAP and WINDSAT). It has been shown that the high winds over the extremely severe TC AMPHAN was very well estimated by SMAP wind products. In addition to wind speed, the SMAP estimated critical wind radii estimates (R34, R50 and R64) for all its passes over TC AMPHAN have been also presented. These products are very useful for assessing the cyclone related damage assessment during its landfall.

The future scope of the works include the analysis of satellite estimates using the final products which is generated after 1-2 month delayed mode.

References

1. Brand, S., Buenafe, C. A. and Hamilton, H. D. (1981). Comparison of tropical cyclone motion and environmental steering. Mon Wea Rev 108:908-909.

2. Chan, J.C.L. and Williams, R.T. (1987). Analytical and numerical studies of the beta-effect in tropical motion. J Atmos Sci 44:1257-1265.

3. Frank, Neil L., Husain, S. A., 1971. The Deadliest Tropical Cyclone in History. *Bull. Amer. Meteor. Soc*., 52, 438–445.

4. Heming J. T. (1994). Keeping an eye on the hurricane -Verification of tropical cyclone forecast tracks at the UK Meteorological Office. NWP Gazette,1, No.2, pp.3 -8.

5. Hoover, B.T. and Morgan M.C. (2006). Effects of cumulus parameterization on tropical cyclone potential vorticity structure and steering flow. Preprints of the 27th AMS Conference on Hurricanes and Tropical Meteorology. April 23-28 Monterey, CA, paper 8B.5.

6. IMD Report, (2015a). Cyclonic Storm, ASHOBAA over the Arabian Sea (07-12 June 2015): A Report. Cyclone Warning Division, India Meteorological Department, New Delhi. June 2015.

7. IMD Report, (2015b). Extremely Severe Cyclonic Storm, CHAPALA over the Arabian Sea (28 October - 4 November, 2015): A Report. Cyclone Warning Division, India Meteorological Department, New Delhi. December 2015.

8. IMD Report, (2015c). Extremely Severe Cyclonic Storm, MEGH over the Arabian Sea (05 - 10 November, 2015): A Report. Cyclone Warning Division, India Meteorological Department, New Delhi. December 2015.

9. IMD Report, (2018). Cyclonic Storm “Daye” over eastcentral Bay of Bengal and adjoining Myanmar (19-22 September 2018): Summary. Regional Specialised Meteorological Centre-Tropical Cyclones, New Delhi, India Meteorological Department, New Delhi. October 2018.

10. IMD Report, (2018). Very Severe Cyclonic Storm “Titli” over eastcentral Bay of Bengal (08-13 October 2018): Summary. Regional Specialised Meteorological Centre-Tropical Cyclones, New Delhi, India Meteorological Department, New Delhi. October 2018.

11. Jaiswal, N., Kishtawal, C. M., Bhomia, S. and Pal, P. K. (2016). Multi-model ensemble based probabilistic prediction of tropical cyclogenesis using TIGGE Model Forecasts. Meteorology and Atmospheric Physics. DOI 10.1007/s00703-016-0436-2.

12. Jaiswal, N., and Kishtawal, C. M., (2011a). Prediction of Tropical Cyclogenesis Using Scatterometer Data. IEEE Transaction on Geoscience and Remote Sensing, vol. 49, Issue 12, pp. 4904 – 4909.

13. Jaiswal, N., and Kishtawal, C. M., (2011b). Automatic Determination of Center of Tropical Cyclone in Satellite-Generated IR Images. IEEE Geoscience and Remote Sensing Letters. vol. 8, No. 3, pp. 460-463.

14. Jaiswal, N., and Kishtawal, C. M., (2012). Objective Detection of Center of Tropical Cyclone in Remotely Sensed Infrared Images. IEEE Journal of Selected Topics in Applied Earth Observations and Remote Sensing. DOI.10.1109/JSTARS.2012.2215016.

15. Jaiswal, N., Kishtawal, C. M., and Pal, P. K., (2013). Prediction of Tropical Cyclogenesis in North Indian Ocean using OSCAT Data. Meteorology Atmospheric Physics, vol. 119, pp. 137–149.

16. Kotal S., Kundu P. and Bhomick, S. K. (2009). Analysis of cyclogenesis parameter for developing and nondeveloping low-pressure systems over the Indian Sea.

17. Kotal S., and Bhattacharya, (2013). Tropical cyclone Genesis Potential Parameter (GPP) and it's application over the north Indian Sea. Mausam 64(1):149-170.

18. Singh, Sanjeev Kumar, Kishtawal, C.M, and Pal, P. K. (2012a). Track prediction of Indian Ocean cyclones using Lagrangian advection model. Nat. Hazards, Vol.63, no.3, 62:745-778.

19. Singh, S. K., Kishtawal, C. M., Jaiswal, N., Singh, R. and P. K. Pal, (2012b). Impact of Vortex-Removal from Environmental Flow in Cyclone Track Prediction using Lagrangian Advection Model. Meteorology Atmospheric Physics, vol. 117, pp. 103–120.

20. Wentz, F.J., L.Ricciardulli, C.Gentemann, T. Meissner, K.A. Hilburn, J. Scott, 2013: Remote Sensing Systems Coriolis WindSat Daily Environmental Suite on 0.25 deg grid, Version 7.0.1. Remote Sensing Systems, Santa Rosa, CA. Available online at www.remss.com/missions/windsat.